For example, mice lacking gp91, one of the two membrane-bound proteins comprising NADPH oxidase cytochrome $b_{558}$, are susceptible to NASH in the MCD model (47).

### *Adiponectin*

Adiponectin, an adipokine secreted by adipocytes, has insulin-sensitizing actions, as well as potent anti-inflammatory effects. Circulating adiponectin concentrations are decreased in animal models of NASH and ALD (46). Treatment of mice with exogenous adiponectin during ethanol feeding or in the *ob/ob* mouse model of NASH prevents liver injury (46). This protection may be due, at least in part, to the anti-inflammatory effects of adiponectin on KCs in the liver, in that treatment of KCs isolated from ethanol-fed rats with adiponectin normalizes LPS-stimulated TNF-α expression (46) (A18).

### *Cyclic AMP*

Cyclic AMP (cAMP) is an important anti-inflammatory signal in KCs; abnormal regulation of cAMP production during NASH or ALD may contribute to increased inflammatory cytokines in the liver. For example, LPS can decrease the expression of adenylyl cyclase (48) (A24) and chronic ethanol decreases Gs (43) and increases phosphodiesterase 4 (49) in KCs. These combined effects suppress agonist-stimulated cAMP production in KCs, probably contributing to the increased inflammatory cytokine production in both NASH and ALD.

### *Interactions of Kupffer cells with hepatocytes*

KCs, because of their proximity, influence hepatocyte function. KC-derived TNF-α has cytotoxic effects on hepatocytes (42). KC-derived mediators, including ROS and cytokines, are likely critical contributors to hepatic insulin resistance (50) (A20), a characteristic of both ALD and NASH. Finally, KCs influence lipid metabolism in hepatocytes. KC-derived endocannabinoids, interacting with the CB-1 receptor on hepatocytes, contribute to liver injury in response to both ethanol and high-fat diets, at least in part via the regulation of fatty acid synthesis and oxidation (51, 52). Further, arachidonic acid-derived lipid mediators produced by KCs also contribute to hepatic steatosis in the *ob/ob* model of NASH (53) (A21).

## Role of Kupffer cells and infiltrating leucocytes in drug-induced hepatotoxicity

Acetaminophen (APAP) is a safe analgesic at therapeutic levels but overdoses cause liver injury and even liver failure. Studies on the mechanisms of cell death mainly focus on intracellular signalling events (54), but recently, the pathophysiological role of the innate immune response has received more attention (55) (A23).

### *Role of tissue macrophages, natural killer cells and neutrophils in acetaminophen hepatotoxicity*

Based on the beneficial effects of compounds such as gadolinium chloride, which are thought to inactivate KCs, it was hypothesized that tissue macrophages contribute to APAP hepatotoxicity (reviewed in (55)). However, several lines of evidence argue against an involvement of KCs in the injury process. Firstly, the centrilobular area of necrosis is inconsistent with the predominant periportal localization of the most active KCs. Secondly, animals deficient in a functional NADPH oxidase, the main enzyme of phagocytes that produces ROS, show the same APAP-induced oxidant stress and liver damage as wild-type animals (56). Furthermore, elimination of KCs with liposomal clodronate aggravated APAP-induced liver injury presumably due to the lack of anti-inflammatory mediator production (57). These data indicate that KCs are actually beneficial during APAP-induced liver injury because of the prevention of an excessive inflammatory response.

Based on experiments with elimination of natural killer (NK) and natural killer T (NKT) cells, it was concluded that these resident lymphocytes contribute to APAP hepatotoxicity (58). However, a recent study indicated that the involvement of NK and NKT cells is dependent on the use of the solvent dimethyl sulfoxide, which can activate these lymphocytes (59). These findings suggest that NK and NKT cells do not contribute to APAP-induced liver injury unless these cells are activated through independent stimuli before APAP administration. This may have some implications for the susceptibility of individuals to APAP overdose but it appears to be of limited relevance for the general toxicity of APAP.

Neutrophils accumulate in the liver in response to APAP-induced necrosis (60). A number of therapeutic interventions directed against neutrophil functions and recruitment had no effect on the oxidant stress and liver injury during the first 24 h after APAP overdose (56, 60, 61). The only exception to this rule appeared to be pretreatment with a neutropaenia-inducing antibody (62). However, this beneficial effect may be independent of the inhibition of neutrophil cytotoxicity, as the removal of the neutrophils activates KCs and preconditions hepatocytes to the APAP-induced stress (63). In support of this conclusion, the neutropaenia-inducing antibody is not effective if administered after APAP (61).

### *Role of macrophages and neutrophils in regeneration after acetaminophen-induced liver injury*

The main purpose of inflammatory cell recruitment into the liver after extensive cell necrosis is to remove dead cells. Necrotic hepatocytes are replaced by dividing hepatocytes closest to the area of necrosis (64). In addition to promoting cell division in healthy hepatocytes, the removal of necrotic cells is critical for the regeneration to be successful. Thus, neutrophils and monocyte-derived macrophages migrate into the necrotic areas and dissolve it. The recruitment of macrophages into the liver is triggered mainly by the formation of monocyte chemoattractant protein 1 (MCP-1), which is generated by macrophages and hepatocytes in the area of injury (65). The receptor for MCP-1 is expressed on infiltrating macrophages (65). Mice deficient in MCP-1 or its receptor have the same initial injury after APAP overdose but show a delayed regenerative response (65). These data suggest that newly recruited macrophages are important for regeneration. In contrast to the critical role of oxidant stress in phagocyte cytotoxicity, the process of necrotic cell removal does not require ROS as animals deficient in a functional NADPH oxidase show a similar regenerative response as wild-type animals (A23). Future studies are needed to elucidate whether these phagocytes are also involved in regulating cell cycle activation and the division of healthy hepatocytes around the area of necrosis.

## Hepatic stellate cells

### Storage of vitamin A as a function of stellate cells

Hepatic stellate cells store about 80% of the body's total vitamin A as retinyl esters (RE) in their lipid droplets (LDs) and play pivotal roles in the regulation of vitamin A homeostasis. HSCs take up retinol from blood by receptor-mediated endocytosis and store vitamin A mainly as retinyl palmitate in LDs in their cytoplasm, and secrete retinol–retinol-binding protein complex into the blood. Unlike adipocytes, HSCs are not involved in energy storage, but they represent a particular cell population specialized in maintaining the concentration of vitamin A in the bloodstream within the physiological range. Under pathological conditions such as liver fibrosis, HSCs lose their LDs and RE (66).

It has been reported that LDs in adipocytes are surrounded by PAT proteins, which were named after perilipin, adipocyte differentiation-related protein (ADRP)/adipophilin and TIP47. In this symposium, Yoshikawa *et al.* (A32) reported the expression of ADRP, and TIP47 around LDs of HSCs. ADRP localized around LDs emitting vitamin A-autofluorescence in quiescent HSCs and the culture-activated HSCs administered with retinol, while TIP47 did not localize around the LDs but diffusely localized in the cytosol in quiescent HSCs, although the colocalization of TIP47 and LDs was observed in activated HSCs. These data suggested that the different palmitoyl acyl transferase (PAT) proteins play specific roles during the formation and maturation of LDs in HSCs. Recently, Straub *et al.* (67) demonstrated that, in the normal liver, PAT proteins were colocalized with the vitamin A-autofluorescence of LDs of HSCs, while in the steatotic liver, ADRP and TIP47 were expressed in LDs of HSCs and additionally in LDs of steatotic hepatocytes. Taken together, the dynamic changes of PAT proteins in HSCs will provide us with considerable knowledge to help in our understanding of the mechanisms leading to the formation and loss of LDs containing vitamin A.

Lecithin: retinol acyltransferase (LRAT) is a retinol esterification enzyme, and it is markedly activated especially in HSCs. Cellular retinol-binding protein-1 (CRBP-1) also mediates retinoid metabolism, and retinol-bound CRBP-1 is a substrate of LRAT. Nagatsuma *et al.* (68) demonstrated that LRAT may be an excellent alternative marker to identify quiescent HSCs as well as CRBP-1 in the normal liver (A34). In the fibrotic/cirrhotic liver, the different patterns of expression for LRAT and α-smooth muscle actin (SMA) facilitated the differentiation between various subsets of fibroblast-like cells involved in fibrogenesis. They also revealed that LRAT was mainly distributed in the rough endoplasmic reticulum and multivesicular bodies of HSCs. The upstream regulatory mechanisms of the expressions of LRAT and CRBP-1, which are retinoic acid-responsive genes, were demonstrated by Mezaki *et al.* (69) in this symposium (A31). Nagatsuma *et al.* reported the co-expression of LRAT and CRBP-1 in the polar bear liver, which was compared with that in human liver. The interaction between LRAT and CRBP-1 could play an important role in the unique vitamin A storage function of HSCs. The cells expressing both LRAT and CRBP-1 were recognized as the functional quiescent HSCs concerned with vitamin A metabolism.

### Comparative biology and stellate cells

To demonstrate the origin of hepatic and extrahepatic SCs in phylogeny, vitamin A and vitamin A-storing cells were investigated in arrowtooth halibut (*Atheresthes evermanni*) (70), lamprey (*Lampetra japonica*) (71) and ascidian (*Halocynthia roretzi*) (72). In the arrowtooth halibut, the highest concentration of stored vitamin A was present in SCs in the pyloric cecum, a teleost-specific organ protruding from the intestine adjacent to the pylorus. Considerable amounts of vitamin A were also stored in SCs in the intestine and liver. In the lamprey, vitamin A was stored in SCs in the intestine, liver, kidney, gill and heart. In the ascidian, retinal is the essential form of vitamin A for storage, and no SCs were observed. Thus, the distribution of SCs with vitamin A-storing capacity differs between mammalian and non-mammalian vertebrates, suggesting that the SCs appeared in the lamprey, and the vitamin A-storing site has shifted during vertebrate evolution.

The bile ducts of larval lamprey degenerate and disappear during metamorphosis, so that no bile duct is observed in the adult liver, which offers a valuable model for studying the liver pathogenesis of human biliary atresia. Miura *et al.* (A42) reported the microstructural analyses of the bile duct degeneration of the lamprey in larval and spawning stage. In larval lamprey, bile canaliculi, intra- and extrahepatic bile ducts, and gall bladder were clearly observed. Apoptotic cells were detected in the epithelium of extrahepatic bile ducts in the latter larval stage of larva. Convoluted bile ducts were surrounded by fibrous deposits of extracellular matrix (ECM) components, where sinusoids were abundant. The HSCs in the perisinusoidal space stored LDs, and several liver parenchymal cells constructed bile canaliculi. In the adult lamprey, the entire biliary system and thick periductal fibrosis disappeared. HSCs containing large quantities of vitamin A and hepatic parenchymal cells with large amount of LDs were observed. However, neither was accompanied by hepatic fibrosis or cirrhosis. These results strongly suggest that the degeneration and disappearance of bile ducts in the lamprey were caused by apoptosis of the bile duct epithelium during metamorphosis when the larvae transformed into the adults. The HSCs were probably responsible for the fibrosis that accompanies the degeneration of bile ducts.

To examine the characteristics of ECM components supporting the sinusoidal wall (scaffolding function) of the liver, the livers of two frozen baby mammoths that died about 40 000 years ago and were buried in permafrost in Siberia, were analysed by Senoo *et al.* (A41). The livers were preserved at gross anatomical and histological levels. The ultrastructure of ECM components, namely the fibrillar structure showing a characteristic pattern of cross striation and basement membrane structure, were clearly demonstrated by transmission and scanning electron microscopy. Type I and type IV collagens were shown in ECM components by immunofluorescence. These findings suggested that the three-dimensional structure of ECM was important for maintaining the gross and histological morphology of the sinusoidal wall in the liver. Thus, comparative biology and phylogeny of HSCs and the liver are indicative and useful for the research of the hepatic sinusoid.

### Regulation of hepatic stellate cell activation

Several recent reports have indicated that hepatic fibrosis and even cirrhosis may regress (73, 74). These observations have toppled the established theory that cirrhosis is an incurable liver disease, particularly from a pathological point of view, and has increased the enthusiasm for developing antifibrogenic therapies. In experimentally induced liver fibrosis in rodents, the cessation of further liver injury by stopping hepatotoxin administration results in fibrosis regression, usually mediated by the reduction of tissue inhibitor of matrix metalloproteinase-1


Liver International (2009)

and apoptosis of HSCs. In humans, the spontaneous resolution of liver fibrosis can occur after successful treatment of the underlying disease. In particular, chronic hepatitis C virus infection has been studied most extensively, and interferon (IFN) therapy with viral eradication results in fibrosis improvement. Among IFNs, IFN-γ is the strongest inhibitor of HSC activation, as revealed by its inhibitory effect on collagen synthesis and α-SMA expression (75). In this symposium, Maubach *et al.* (A27) (76) reported that IFN-γ induces the class II transactivator, the invariant chain (CD74), the major histocompatibility complex (MHC) class II molecules and cathepsin S in activated rat HSCs, indicating that IFN-γ is an important regulator in antigen presentation in HSCs. Other recent studies have indicated that HSCs in culture undergo apoptosis via pentapeptide GRGDS (Gly-Arg-Gly-Asp-Ser), nerve growth factor (NGF), a high dose of sphingosine-1-phosphate, gliotoxin, and so on. The regulation of HSC activation by C-reactive protein, an acute-phase reactant that participates in inflammatory responses and is produced by hepatocytes, has shed a new light on the local cell–cell interactions (A39).

Tsukamato *et al.* (A28) showed that transcriptional regulation essential for adipocyte differentiation is required for the maintenance of HSC quiescence. Quiescent HSCs express peroxisome proliferators-activated receptor (PPAR-γ), CCAAT/enhancer-binding protein (C/EBP)-α, -β, -δ, liver X receptor α (LXR-α) and sterol-regulatory element-binding protein-1c (SREBP-1c), which are adipogenic transcription factors and are downregulated by the HSC activation process (77). Activated HSCs show phenotypic reversal by the forced expression of PPAR-γ or SREBP-1c, or by the treatment of cells with the adipocyte differentiation cocktail MDI (methylxanthin, dexamethasone and insulin). They further reported the involvement of a new class of antiadipogenic factors: the Wnt family of proteins. That is, canonical (Wnt3a and 10b) and non-canonical (Wnt4 and 5) Wnts, their receptors (Frizzeled-1 and -2) and coreceptors [lipoprotein receptor-related protein (LRP) 6 and Ryk] are induced in activated rat HSC *in vitro* and *in vivo*. Most interestingly, Wnt antagonism using the LRP coreceptor antagonist Dkk-1 restores both the expression of the adipogenic transcription factors listed above and the HSC quiescence (78).

Another interesting transcription factor is early growth response 1 (Egr-1). Egr-1 is an immediate early gene that is both rapidly and transiently induced in response to a variety of stress factors. It also regulates the expression of genes involved in the fibrotic process including basic fibroblast growth factor (bFGF), VEGF, TGF-β and platelet-derived growth factor (PDGF). Pritchard *et al.* (A35) demonstrated the development of enhanced fibrosis and augmented α-SMA expression after carbon tetrachloride injection in Egr-1$^{-/-}$ mice compared with wild-type mice. These data suggest that Egr-1 plays a protective role in fibrosis.

In addition to vitamin A, vitamin E proved to be absorbed and accumulated in HSCs. Vitamin E is composed of eight different forms: α-, β-, γ- and δ-tocopherols and -tocotrienols. Since the discovery of vitamin E in 1922, studies on tocopherols and tocotrienols have focused mainly on their antioxidant properties. Recently, the non-antioxidant functions of vitamin E were verified, and it was shown to deactivate protein kinase C in smooth muscle cells, lower cholesterol level, inhibit platelet adhesion and exhibited anticancer property (79). Furthermore, tocopherols reportedly promote the transciption of Bcl2, α-tocopherol transfer protein, cytochrome P450, tropomyosin and PPAR-γ, and inhibit that of CD36, SR-BI, collagen α1, matrix metalloproteinase-1 (MMP-1), MMP-19, E-selectin, ICAM-1, integrins and cyclins D1 and E (80). In this context, Yamaguchi *et al.* showed the inhibitory effects of the four tocopherols and tocol on HSC proliferation and the induction of apoptosis (A36). The addition of δ-tocopherol and tocol to culture-activated HSCs resulted in marked morphological changes leading to detachment from a substratum. According to these observations, the authors suggested that vitamin E would be a promising candidate for the treatment of hepatic fibrosis and liver cirrhosis.

## Transforming growth factor-β as a key regulator of hepatic stellate cell activation

Transforming growth factor (TGF)-β is a key regulatory molecule for ECM metabolism, and it functions as an autocrine and a paracrine mediator (66). Cellular sources of TGF-β1 are diverse, including HSCs, KCs, hepatocytes, LSECs and platelets. Proteolytic cleavage of latent TGF-β-binding protein is a prerequisite for the release and generation of bioactive (mature) TGF-β, which is induced by urokinase plasminogen activator or tissue plasminogen activator. The impact of TGF-β1 on liver fibrosis has been well documented via the marked attenuation of liver fibrosis development using the soluble type II TGF-β receptor and in a model of adenoviral delivery of the dominant-negative TGF-β receptor. The role of the Smad cascade in TGF-β signalling has been characterized in HSCs (68). Furthermore, bone morphogenic protein-7 antagonizes TGF-β signalling through Smad1/5/7 and Id-2, and thereby suppresses collagen gene expression (81).

In this symposium, Kojima S *et al.* (A40) showed that TGF-β is activated by proteases such as plasmin (PLN) and plasma kallikrein (PLK) on the surface of HSCs during pathogenesis of liver fibrosis and that blockage of these activation reactions with a protease inhibitor, camostat mesilate, prevented the disease development. They further showed that PLN and PLK cleaved between $K^{56}$–$L^{57}$ and $R^{58}$–$L^{59}$, respectively, within the latency-associated protein portion of human latent TGF-β1; this finding indicates a novel detection system of TGF-β activation *in vivo* using the antibodies recognizing PLK cut ends. They further demonstrated that peptides containing protease cleavage sites as well as their decoy peptide effectively suppressed the TGF-β activation reaction and prevented the activation of HSCs in culture.

## The hepatic stellate cell as a principal player in liver fibrosis

Hepatic stellate cells, which reside in Disse's space in close contact with both LSECs and hepatocytes, play multiple roles in hepatic pathophysiology (82) Quiescent HSCs represent a vitamin A-storing phenotype and metabolize a small amount of basement membrane-forming laminin and type IV collagen. When hepatitis is induced by iron overload, alcohol consumption, infection with hepatitis viruses B or C, NASH, autoimmune hepatitis and bile duct obstruction, local inflammation and damaged hepatocytes activate HSCs. This process is triggered by oxidative stress due to lipid hydroperoxide and reactive aldehyde generated in and released from damaged or apoptotic hepatocytes and KCs, via the paracrine stimulation of PDGF-BB, insulin-like growth factor-1 and TGF-β derived from sinusoidal cells, platelets and infiltrating leucocytes, and by the production of a splice variant of cellular fibronectin (EIIIA isoform) (83–86). Activated HSCs change their phenotype to 'myofibroblast'-like cells that produce increased

amounts of types I and III collagens, show augmented contractility accompanied by the expression of α-SMA and the production of ET-1, secrete TGF-β and MCP-1, lose retinoid and exhibit active apoptosis. Transcriptional activation by Kruppel-like factor 6, activator protein 1 and C/EBP enhances gene expression regulating ECM accumulation (87).

### Involvement of iron in hepatic stellate cell function and liver fibrosis

The role of iron in the hepatic pathophysiology has long been studied in fields of haemochromatosis and alcoholic liver injury (88). Recently, an unusual accumulation of iron in the liver has also been observed in chronic hepatitis C and NASH. The activation process of HSCs is triggered by oxygen free radicals, including hydrogen peroxide ($H_2O_2$), which can be produced by the Fenton reaction of $Fe^2+H_2O_2 \rightarrow Fe^3+HO^-+HO^{\cdot}$. Free iron induces the production of TNF-α and TGF-β1 and nuclear factor-κB (NF-κB) activation in hepatic macrophages (89). The free radicals generated induce lipid peroxidation, DNA breakage and 8-hydroxy-2′-deoxyguanosine formation, resulting in tissue damage and DNA mutagenesis (90). Thus, iron is also a key molecule for liver fibrogenesis.

Ferritin is an iron-binding protein that is composed of 24 individual proteins of either heavy (H) or light (L) subtypes and is important for iron homeostasis. Although it is well known that serum ferritin level increases in the course of liver inflammation, the exact reason for this elevation is unclear. Ruddel *et al.* (A33) identified the role of T-cell immunoglobulin and mucin domain-2 (Tim-2), which is a receptor for H ferritin endocytosis, in HSC activation. Tim-2 mRNA and proteins were present in HSCs and were weakly induced in the process of activation. The incubation of HSCs with tissue ferritin augmented the phosphorylation of the PI3-kinase target motif YXXM, protein kinase Cz (PKCz), p42/p44 mitogen-activated protein kinase and IKK, leading to the activation of NF-κB. These data suggest a novel bioactive function of ferritin independent of its binding to iron.

Kawada *et al.* (91) discovered a new iron-binding protein, cytoglobin, the fourth globin in mammals by proteomics analysis of HSC activation. Cytoglobin shows amino acid sequence homology with vertebrate myoglobin, haemoglobin and neuroglobin. Cytoglobin is uniquely localized in fibroblast-like cells in splanchnic organs, namely vitamin A-storing cell lineages, including pancreatic SCs, reticular cells in the spleen and mesangial cells in the kidney (92). The oxygen- and carbon monoxide-binding equilibrium and kinetic properties are nearly identical between cytoglobin and myoglobin, indicating that cytoglobin may convey oxygen to the mitochondria of actin-rich non-muscle cells to facilitate cell contraction (A25). On the other hand, a recent report by Xu *et al.* (93) demonstrated the anti-oxidative and cytoprotective action of cytoglobin by over-expressing this protein using adenovirus-associated gene transfer in the rat liver injured by carbon tetrachloride injection.

### Are hepatic stellate cells a pure single population?

As stated above, the contribution of HSCs to the hepatic fibrotic process is well recognized. However, recently, several lines of evidence have pointed out the heterogeneity of hepatic 'myofibroblasts'. In other words, it is now questionable whether activated HSCs are identical to myofibroblasts (94). Both activated HSCs and myofibroblasts express α-SMA and collagens α1(I) and α1(III). However, desmin, P100 and α2-macroglobulin are expressed in activated HSCs, but not in myofibroblasts. Additonally, fibulin-2, gremlin, cardiac troponin T and lumican are present in myofibroblasts, but absent in activated HSCs. A recent study using transgenic mice that express the red fluorescent protein and enhanced green fluorescent protein reporter genes under the direction of the mouse α-SMA and collagen α1(I) promoter/enhancer, respectively, demonstrated that there are at least three myofibroblastic populations: α-SMA-only expressing cells, collagen-only expressing cells and dual-positive cells (95). Activated and myofibroblast-like HSCs are derived from vitamin A-storing quiescent HSCs. In contrast, the origin of myofibroblasts remains controversial: they may be derived from portal fibroblasts, vitamin A-free HSCs or hepatic stem cells. Fascin has been proposed as a novel marker that distinguishes human HSCs from portal fibroblasts (A57). The theory of epithelial–mesenchymal transition has brought about further confusion in this field.

The participation of cells in the blood in the hepatic fibrotic process has additionally been proposed. These cells are generated from bone marrow-derived mesenchymal cells or circulating fibrocytes and may serve as a substantial fraction of the fibrogenic cell population in the liver during chronic injury. However, there also exists some controversy; bone marrow-derived cells may provide fibrogenic cells, while bone marrow-derived endothelial cell progenitor cells can be antifibrogenic. Hepatocyte growth factor (HGF) gene transfer accelerated the recruitment of bone marrow-derived mesenchymal cells into the liver, increasing the gelatinase activity in the fibrotic area (Iimuro *et al.*, A61). On the other hand, Witters *et al.* (A37) described an impairment of blood platelet function in cholestatic liver disease. Because platelets are one of the major sources of growth factors, such as PDGF, HGF, prostaglandins and platelet-activating factors, involved in inflammatory and fibrotic processes, analysis of the function of platelets in liver fibrosis should be considered further. Ogawa *et al.* (A38) emphasized the involvement of senescent erythrocytes in the pathogenesis of a rabbit model of steatohepatitis.

## Immunology (A44)

The cells of the hepatic sinusoid have a strategic position to interact with immune cells passing with the blood stream through the hepatic sinusoids. Interaction is further facilitated by the narrow sinusoidal diameter, slow and irregular blood flow as well as low perfusion pressure. The liver is known as an immune regulatory organ, which contributes to the elimination of pathogens from the circulation but at the same time favoring the induction of immune tolerance rather than adaptive immunity (96, 97). At the ISCHS-meeting in Tromsø, various groups presented the involvement of KCs in innate immune reactions that are critical for the development of drug-induced liver disease (please see symposium session V). KCs have also been shown to contribute to bystander-hepatitis during extrahepatic influenza infection (98) and are known to engage in a cross-talk with hepatic NK cells upon contact with TLR ligands (99). These interactions often lead to an increased expression of cytokines with effector function such as TNF-α, and thereby promote innate immunity against infectious microorganisms or induce liver damage. Other cell populations such as NK cells, NKT cells and γδ-T cells represent significant populations in the liver but their contribution to local immune regulation is currently not well defined, although their role in antiviral defence has been demonstrated recently (100). These cell

populations either recognize pathogens or altered cells through genetically conserved surface receptors or express a skewed repertoire of T-cell receptors recognizing their antigen in the context of the evolutionaryly conserved CD1 molecule. Nevertheless, *in vivo* imaging revealed that NKT cells continuously patrol the hepatic sinusoids and are arrested upon specific recognition of a cognate ligand, α-galactosyl-ceramide, which is presented in a CD1-restricted fashion (101). Certainly, these innate immune cells play a key role in local pathogen defense in the liver but the exact cellular and molecular mechanisms involved remain to be identified.

An important link between innate and adaptive immune responses is the expression of chemokines, which recruit lymphocytes with effector functions. The Adams group in Birmingham has recently revealed that chemokine CCL25 recruits pathogenic $CCR9^+$ CD8 T cells into the liver in patients with primary sclerosing cholangitis (102). These findings further demonstrate an important connection between the gut and the liver, as hepatic recirculation of T cells initially primed in the intestinal tract is involved in the manifestation of hepatic autoimmunity (103). Also, expression of chemokines by LSECs is important for the transendothelial migration of T cells and subsequent development of local effector function (104, 105).

Induction of antigen-specific tolerance in CD8 T cells has been attributed to hepatic cell populations that bear the capacity to function as antigen-presenting cells. Besides hepatocytes, which represent the most prominent hepatic cell population and induce deletional tolerance in CD8 T cells (106, 107), KCs (108), HSCs (109) and LSECs have been implicated in mediating T-cell tolerance (110). KCs bear the capacity to present antigen on MHC class I and MHC class II molecules to CD8 and CD4 T cells respectively. Using a model of murine liver transplantation, Klein *et al.* (79) reported that KCs can be divided in a bone marrow derived and an organ-resident cell population with distinct functional and phenotypic characteristics. The group of Yamamoto *et al.* further expanded our knowledge on organ-resident KCs by reporting that this cell population constitutes a fixed proportion of the entire population of KCs and therefore presumably depends on local signals for survival and growth (A19). Further research is required in order to clearly assign particular functional properties to this organ-resident KC population.

It is accepted that the initial antigen-specific stimulation of naïve CD8 T cells in the liver determines their subsequent functional capacity, i.e. tolerance, whereas extrahepatic priming of T cells in the secondary lymphatic tissue leads to the development of T-cell immunity that upon antigen-recognition in the liver can develop into autoimmunity (107). Bertolino *et al.* (111) reported that ubiquitous antigen-presentation on MHC class I molecules leads to rapid hepatic recruitment of circulating naïve CD8 T cells. Knolle *et al.* (A44) presented data that LSECs cross-present circulating antigens to naïve CD8 T cells, leading to a rapid and liver-specific recruitment of antigen-specific T cells to the liver. The consequence of antigen-specific retention is an initial stimulation of naïve CD8 T cells but ultimately the development of CD8 T-cell tolerance. T-cell tolerance induced by antigen-presenting LSEC is characterized by mutual upregulation of co-inhibitory molecules on LSEC (B7H1) and the interacting T cells (PD1). The balance of co-inhibitory and costimulatory signals determines whether LSEC induce T-cell tolerance. $B7H1^{-/-}$ LSEC that fail to trigger PD1 stimulation also fail to induce T-cell tolerance, whereas additional costimulation through CD28 overrides tolerogenic signals promoting effector cell generation (112). Tolerance induction by LSEC has been shown to play a role in oral tolerance and development of tumour-specific tolerance following systemic tumour cell distribution (113, 114). Collectively, the early steps in recruiting naïve T cells to the liver and the functional outcome of these physical interactions influence subsequent systemic immune responses. Furthermore, cross-talk between liver sinusoidal cells and tumour cells may enhance the hepatic metastasis of circulating tumour cells, as was reported by Vidal-Vanaclocha *et al.* at this meeting (A45).

Taken together, an understanding of the cellular and molecular mechanisms determining the local regulation of immune responses in the liver will not only further our knowledge on the pathophysiological principles underlying persistent viral infection of the liver but will also allow us to develop therapeutic principles to deliberately increase tolerance during autoimmunity or to increase immunity in persistent viral infection or cancer.

## Tumour/metastasis

### Contribution of sinusoidal cells to hepatic metastasis

This section describes the contribution of sinusoidal cells to metastatic cancer cell regulation. Four phases of the metastasis process have been considered: (a) the microvascular phase of liver-infiltrating cancer cells, including mechanisms of intravascular arrest, death and survival of cancer cells within the inflammatory micro-environment of tumour-activated sinusoidal cells and immune escape mechanisms; (b) the intralobular micrometastasis phase, including growth activation of cancer cells and stromal cell recruitment into avascular micrometastases; (c) the angiogenic micrometastasis phase, including endothelial cell recruitment and blood vessel formation supported by proangiogenic myofibroblasts; and (d) the established hepatic metastasis phase, whose clinical significance is still affected by intratumoral stroma, blood vessel density, tumour-infiltrating lymphocytes and gene expression profile of cancer cells.

### The microvascular phase of liver-infiltrating cancer cells

The hepatic metastasis process begins with the microvascular retention of circulating cancer cells. Mechanical stress suffered by cancer cells on entry and residence in the hepatic microvasculature contributes to cancer cell death. Infiltrating cancer cells can induce the obstruction of sinusoids, leading to transient micro-infarcts that damage hepatic cells. In turn, re-oxygenation of ischaemic sinusoids induces the killing of cancer cells as a result of the release of NO and reactive oxygen intermediates from sinusoidal cells (115, 116). KCs can phagocytose cancer cells and modulate the antitumour immune response by releasing cytotoxic products and immune-stimulating factors activating hepatic NK cells (117, 118). In turn, these cells produce antitumour cytotoxicity via perforin/granzyme-containing granule secretion and death receptor-mediated mechanisms (119). However, some arrested cancer cells can resist and even deactivate antitumour defense mechanisms through several mechanisms: tumour-derived CEA (carcinoembryonic antigen) can prevent cancer cell death by inducing IL-10 to inhibit inducible NO synthase upregulation in sinusoidal cells (120). Expression of MHC class I on cancer cells can also promote immune escape via the negative regulation of hepatic NK cells. The high intracellular content of glutathione can also protect cancer cells from oxidative stress

(116). It was also reported at the symposium (A17) that IL-1-dependent MR upregulation in tumour-activated LSECs inhibits IFN-γ secretion and antitumour cytotoxicity of hepatic lymphocytes. The release of MR-stimulating factors was an immunosuppressant feature induced by ICAM-1-depedent COX-2 in liver-colonizing cancer cells expressing LFA-1. Because IL-1, COX-2 and ICAM-1 inhibitors show antimetastatic effects, it was suggested that MR-dependent hepatic immune suppression constitutes a common mediator for prometastatic effects induced by IL-1, COX-2 and ICAM-1. Liver-infiltrating cancer cells that survive in the microvasculature adhere to hepatic endothelial cells via vascular adhesion receptors regulated by proinflammatory cytokines and $H_2O_2$ (121–123). These microvascular events influence metastasis, and factors that neutralize inflammatory cytokines or adhesion receptors for cancer cells have therapeutic potential (124–126).

### The intralobular micrometastasis phase

Intrasinusoidal cancer cell proliferation is activated by growth factors released from LSEC (122), while extravascular cancer cell proliferation is activated by factors released from tumour-activated perisinusoidal HSCs (127) and hepatocytes. These mechanisms are affected by both the phenotypic heterogeneity of hepatocytes and sinusoidal cells and the gradients of oxygen, hormones and ECM across the liver lobule.

A rich tumour growth-stimulating stroma is recruited into micrometastases before angiogenesis. The main sources of stromal cells are as follows: (a) HSCs (127), which support intralobular micrometastases and are transdifferentiated into myofibroblasts firstly at sites of cancer cell adhesion to LSEC before extravasation (A77) and secondly induced by paracrine factors from extravasated cancer cells. (b) Portal tract fibroblasts, which support perilobular micrometastases and are activated by cancer cells extravasated at terminal portal venules (128). (c) Perimetastatic hepatocytes, which sometimes suffer an epithelial to mesenchymal transition induced by cancer cells and tumour-activated HSCs, and express NGF as reported at the symposium (A46).

### The angiogenic micrometastasis phase

Proangiogenic factors from hypoxic tumour-activated stromal cells and cancer cells contribute to this phase. Endothelial cell migration occurs only towards avascular micrometastases containing a high density of myofibroblasts and not towards those not containing myofibroblasts (127). Both myofibroblasts and endothelial cells colocalize, and their densities consistently correlate in well-vascularized metastases (127). Two predominant angiogenic patterns occur (129), which correlate with the site of metastatic cell implantation, the distinct stromal cell types, the invasion and growth patterns and the treatment resistance (130): (a) Sinusoidal-type angiogenesis occurring in metastases with replacement growth-pattern, where the liver architecture is preserved because cancer cells co-opt the existing network of sinusoids. Here, desmin- and glial fibrillary acidic protein-expressing myofibroblasts suggest their HSC origin (127). (b) Portal-type angiogenesis occurring in metastases with desmoplastic and pushing growth patterns. Here, the liver micro-architecture is not preserved and the growing metastatic tissue is delineated by desmoplastic stroma and compresses the surrounding parenchyma. Here, vimentin- and Thy-1 phenotype-expressing myofibroblasts suggest their portal tract fibroblast origin (128). Specific angiogenic factors produced by sinusoidal- and portal tract-derived myofibroblasts also contribute to angiogenic pattern differentiation (127, 128).

### The established hepatic metastasis phase

Cancer cells can still be micro-environmentally modulated by stromal myofibroblasts and tumour-infiltrating hepatic lymphocytes, including CD4/CD25 regulatory T cells. The high intrahepatic concentration of proinflammatory and immunosuppressant cytokines, angiogenic and stromagenic factors, and soluble adhesion molecules also has regulatory effects on cancer cells, and prognostic implications. Consistent with this molecular micro-environment, remarkable gene expression alterations occur at hepatic metastases in this phase. Some originate at the primary tumours and may support hepatic metastasis, while others are differentially promoted by hepatocytes and hepatic myofibroblasts (A45). Consistent with the tumour proliferation-stimulating activity of sinusoidal cells, around 50% of hepatic metastasis genes regulated by factors from HSC-derived myofibroblasts belonged to the cell cycle-regulation class. Therefore, despite the occurrence of hepatic metastasis genes in the primary tumours, which may predict metastasis risk, tumour-activated hepatic cells may create a micro-environment contributing to the expression of genes operating at advanced phases of the hepatic metastasis process that may have therapeutic implications.

## References


1. Martinez I, Nedredal GI, Oie CI, *et al.* The influence of oxygen tension on the structure and function of isolated liver sinusoidal endothelial cells. *Comp Hepatol* 2008; **7**: 4.
2. DeLeve LD, Wang X, McCuskey MK, McCuskey RS. Rat liver endothelial cells isolated by anti-CD31 immunomagnetic separation lack fenestrae and sieve plates. *Am J Physiol* 2006; **291**: G1187–9.
3. DeLeve LD, Wang X, Hu L, McCuskey MK, McCuskey RS. Rat liver sinusoidal endothelial cell phenotype is maintained by paracrine and autocrine regulation. *Am J Physiol* 2004; **287**: G757–63.
4. Cogger VC, Arias IM, Warren A, *et al.* The response of fenestrations, actin, and caveolin-1 to vascular endothelial growth factor in SK Hep1 cells. *Am J Physiol Gastrointest Liver Physiol* 2008; **295**: G137–45.
5. Yokomori H, Yoshimura K, Funakoshi S, *et al.* Rho modulates hepatic sinusoidal endothelial fenestrae via regulation of the actin cytoskeleton in rat endothelial cells. *Lab Invest* 2004; **84**: 857–64.
6. Carpenter B, Lin Y, Stoll S, *et al.* VEGF is crucial for the hepatic vascular development required for lipoprotein uptake. *Development* 2005; **132**: 3293–303.
7. Le Couteur DG, Fraser R, Hilmer S, Rivory LP, McLean AJ. The hepatic sinusoid in aging and cirrhosis – effects on hepatic substrate disposition and drug clearance. *Clin Pharmacokinet* 2005; **44**: 187–200.
8. Hilmer SN, Cogger VC, Fraser R, *et al.* Age-related changes in the hepatic sinusoidal endothelium impede lipoprotein transfer in the rat. *Hepatology* 2005; **42**: 1349–54.
9. Warren A, Le Couteur DG, Fraser R, *et al.* T lymphocytes interact with hepatocytes through fenestrations in murine liver sinusoidal endothelial cells. *Hepatology* 2006; **44**: 1182–90.
10. Wisse E, Jacobs F, Topal B, Frederik P, De Geest B. The size of endothelial fenestrae in human liver sinusoids: implications for hepatocyte-directed gene transfer. *Gene Ther* 2008; **15**: 1193–9.

11. Smedsrod B, Pertoft H, Gustafson S, Laurent TC. Scavenger functions of the liver endothelial cell. *Biochem J* 1990; **266**: 313–27.
12. Malovic I, Sorensen KK, Elvevold KH, *et al.* The mannose receptor on murine liver sinusoidal endothelial cells is the main denatured collagen clearance receptor. *Hepatology* 2007; **45**: 1454–61.
13. Elvevold K, Simon-Santamaria J, Hasvold H, *et al.* Liver sinusoidal endothelial cells depend on mannose receptor-mediated recruitment of lysosomal enzymes for normal degradation capacity. *Hepatology* 2008; **48**: 2007–15.
14. Melkko J, Hellevik T, Risteli L, Risteli J, Smedsrod B. Clearance of $NH_2$-terminal propeptides of types I and III procollagen is a physiological function of the scavenger receptor in liver endothelial cells. *J Exp Med* 1994; **179**: 405–12.
15. Smedsrod B, Melkko J, Araki N, Sano H, Horiuchi S. Advanced glycation end products are eliminated by scavenger-receptor-mediated endocytosis in hepatic sinusoidal Kupffer and endothelial cells. *Biochem J* 1997; **322**(Part 2): 567–73.
16. McCourt PA, Smedsrod BH, Melkko J, Johansson S. Characterization of a hyaluronan receptor on rat sinusoidal liver endothelial cells and its functional relationship to scavenger receptors. *Hepatology* 1999; **30**: 1276–86.
17. Hansen B, Arteta B, Smedsrod B. The physiological scavenger receptor function of hepatic sinusoidal endothelial and Kupffer cells is independent of scavenger receptor class A type I and II. *Mol Cell Biochem* 2002; **240**: 1–8.
18. Hansen B, Longati P, Elvevold K, *et al.* Stabilin-1 and stabilin-2 are both directed into the early endocytic pathway in hepatic sinusoidal endothelium via interactions with clathrin/AP-2, independent of ligand binding. *Exp Cell Res* 2005; **303**: 160–73.
19. Mousavi SA, Sporstol M, Fladeby C, *et al.* Receptor-mediated endocytosis of immune complexes in rat liver sinusoidal endothelial cells is mediated by Fc gammaRIIb2. *Hepatology* 2007; **46**: 871–84.
20. Takizawa T, Anderson CL, Robinson JM. A novel Fc gamma R-defined, IgG-containing organelle in placental endothelium. *J Immunol* 2005; **175**: 2331–9.
21. Seternes T, Sorensen K, Smedsrod B. Scavenger endothelial cells of vertebrates: a nonperipheral leukocyte system for high-capacity elimination of waste macromolecules. *Proc Natl Acad Sci USA* 2002; **99**: 7594–7.
22. Martin-Armas M, Zykova S, Smedsrod B. Effects of CpG-oligonucleotides, poly I:C and LPS on Atlantic cod scavenger endothelial cells (SEC). *Dev Comp Immunol* 2008; **32**: 100–7.
23. Crossley AC. The ultrastructure and function of pericardial cells and other nephrocytes in an insect: calliphora erythrocephala. *Tissue Cell* 1972; **4**: 529–60.
24. Yoshida M, Nishikawa Y, Omori Y, *et al.* Involvement of signaling of VEGF and TGF-beta in differentiation of sinusoidal endothelial cells during culture of fetal rat liver cells. *Cell Tissue Res* 2007; **329**: 273–82.
25. Keitel V, Reinehr R, Gatsios P, *et al.* The G-protein coupled bile salt receptor TGR5 is expressed in liver sinusoidal endothelial cells. *Hepatology* 2007; **45**: 695–704.
26. Watanabe N, Takashimizu S, Nishizaki Y, *et al.* An endothelin A receptor antagonist induces dilatation of sinusoidal endothelial fenestrae: implications for endothelin-1 in hepatic microcirculation. *J Gastroenterol* 2007; **42**: 775–82.
27. Yokomori H, Yoshimura K, Ohshima S, *et al.* The endothelin-1 receptor-mediated pathway is not involved in the endothelin-1-induced defenestration of liver sinusoidal endothelial cells. *Liver Int* 2006; **26**: 1268–76.
28. Deleve LD, Wang X, Guo Y. Sinusoidal endothelial cells prevent rat stellate cell activation and promote reversion to quiescence. *Hepatology* 2008; **48**: 920–30.
29. Qiao JG, Wu L, Lei DX, Wang L. Insulin promotes sinusoidal endothelial cell proliferation mediated by upregulation of vascular endothelial growth factor in regenerating rat liver after partial hepatectomy. *World J Gastroenterol* 2005; **11**: 5978–83.
30. Falkowska-Hansen B, Falkowski M, Metharom P, Krunic D, Goerdt S. Clathrin-coated vesicles form a unique net-like structure in liver sinusoidal endothelial cells by assembling along undisrupted microtubules. *Exp Cell Res* 2007; **313**: 1745–57.
31. Klein D, Demory A, Peyre F, *et al.* Wnt2 acts as a cell type-specific, autocrine growth factor in rat hepatic sinusoidal endothelial cells cross-stimulating the VEGF pathway. *Hepatology* 2008; **47**: 1018–31.
32. Le Couteur DG, Warren A, Cogger VC, *et al.* Old age and the hepatic sinusoid. *Anat Rec* 2008; **291**: 672–83.
33. Ito Y, Sorensen KK, Bethea NW, *et al.* Age-related changes in the hepatic microcirculation of mice. *Exp Gerontol* 2007; **48**: 789–97.
34. Collardeau-Frachon S, Scoazec J. Vascular development and differentiation during human liver organogenesis. *Anat Rec* 2008; **291**: 614–27.
35. McCuskey RS. The hepatic microvascular system in health and its response to toxicants. *Anat Rec* 2008; **291**: 661–71.
36. Deleve LD. Hepatic microvasculature in liver injury. *Semin Liver Dis* 2007; **27**: 390–400.
37. Cogger VC, Muller M, Fraser R, *et al.* The effects of oxidative stress on the liver sieve. *J Hepatol* 2004; **41**: 370–76.
38. McCuskey RS, Ito Y, Robertson GR, *et al.* Hepatic microvascular dysfunction during evolution of dietary steatohepatitis in mice. *Hepatology* 2004; **40**: 386–93.
39. Ohmura T, Enomoto K, Satoh H, Sawada N, Mori M. Establishment of a novel monoclonal antibody, SE-1, which specifically reacts with rat hepatic sinusoidal endothelial cells. *J Histochem Cytochem* 1993; **41**: 1253–7.
40. Tokairin T, Nishikawa Y, Doi Y, *et al.* A highly specific isolation of rat sinusoidal endothelial cells by the immunomagnetic bead method using SE-1 monoclonal antibody. *J Hepatol* 2002; **36**: 725–33.
41. Rivera CA. Risk factors and mechanisms of non-alcoholic steatohepatitis. *Pathophysiology* 2008; **15**: 109–14.
42. Thurman II RG. Alcoholic liver injury involves activation of Kupffer cells by endotoxin. *Am J Physiol* 1998; **275**: G605–11.
43. Nagy LE. Recent insights into the role of the innate immune system in the development of alcoholic liver disease. *Exp Biol Med (Maywood)* 2003; **228**: 882–90.
44. Hritz I, Mandrekar P, Velayudham A, *et al.* The critical role of toll-like receptor (TLR) 4 in alcoholic liver disease is independent of the common TLR adapter MyD88. *Hepatology* 2008; **48**: 1224–31.
45. Zhao XJ, Dong Q, Bindas J, *et al.* TRIF and IRF-3 binding to the TNF promoter results in macrophage TNF dysregulation and steatosis induced by chronic ethanol. *J Immunol* 2008; **181**: 3049–56.
46. Huang H, Park PH, McMullen MR, Nagy LE. Mechanisms for the anti-inflammatory effects of adiponectin in macrophages. *J Gastroenterol Hepatol* 2008; **23**(Suppl. 1): S50–3.
47. dela Pena A, Leclercq IA, Williams J, Farrell GC. NADPH oxidase is not an essential mediator of oxidative stress or liver injury in murine MCD diet-induced steatohepatitis. *J Hepatol* 2007; **46**: 304–13.
48. Risoe PK, Wang Y, Stuestol JF, *et al.* Lipopolysaccharide attenuates mRNA levels of several adenylyl cyclase isoforms in vivo. *Biochim Biophys Acta* 2007; **1772**: 32–9.
49. Gobejishvili L, Barve S, Joshi-Barve S, McClain C. Enhanced PDE4B expression augments LPS-inducible TNF expression in ethanol-primed monocytes: relevance to alcoholic liver disease. *Am J Physiol Gastrointest Liver Physiol* 2008; **295**: G718–24.

50. Leclercq IA, Da Silva Morais A, Schroyen B, Van Hul N, Geerts A. Insulin resistance in hepatocytes and sinusoidal liver cells: mechanisms and consequences. *J Hepatol* 2007; **47**: 142–56.
51. Jeong WI, Osei-Hyiaman D, Park O, *et al.* Paracrine activation of hepatic CB1 receptors by stellate cell-derived endocannabinoids mediates alcoholic fatty liver. *Cell Metab* 2008; **7**: 227–35.
52. Osei-Hyiaman D, DePetrillo M, Pacher P, *et al.* Endocannabinoid activation at hepatic CB1 receptors stimulates fatty acid synthesis and contributes to diet-induced obesity. *J Clin Invest* 2005; **115**: 1298–305.
53. Lopez-Parra M, Titos E, Horrillo R, *et al.* Regulatory effects of arachidonate 5-lipoxygenase on hepatic microsomal TG transfer protein activity and VLDL-triglyceride and apoB secretion in obese mice. *J Lipid Res* 2008; **49**: 2513–23.
54. Jaeschke H, Bajt ML. Intracellular signaling mechanisms of acetaminophen-induced liver cell death. *Toxicol Sci* 2006; **89**: 31–41.
55. Jaeschke H. Role of inflammation in the mechanism of acetaminophen-induced hepatotoxicity. *Expert Opin Drug Metab Toxicol* 2005; **1**: 389–97.
56. James LP, McCullough SS, Knight TR, Jaeschke H, Hinson JA. Acetaminophen toxicity in mice lacking NADPH oxidase activity: role of peroxynitrite formation and mitochondrial oxidant stress. *Free Radic Res* 2003; **37**: 1289–97.
57. Ju C, Reilly TP, Bourdi M, *et al.* Protective role of Kupffer cells in acetaminophen-induced hepatic injury in mice. *Chem Res Toxicol* 2002; **15**: 1504–13.
58. Liu ZX, Govindarajan S, Kaplowitz N. Innate immune system plays a critical role in determining the progression and severity of acetaminophen hepatotoxicity. *Gastroenterology* 2004; **127**: 1760–74.
59. Masson MJ, Carpenter LD, Graf ML, Pohl LR. Pathogenic role of natural killer T and natural killer cells in acetaminophen-induced liver injury in mice is dependent on the presence of dimethyl sulfoxide. *Hepatology* 2008; **48**: 889–97.
60. Lawson JA, Farhood A, Hopper RD, Bajt ML, Jaeschke H. The hepatic inflammatory response after acetaminophen overdose: role of neutrophils. *Toxicol Sci* 2000; **54**: 509–16.
61. Cover C, Liu J, Farhood A, *et al.* Pathophysiological role of the acute inflammatory response during acetaminophen hepatotoxicity. *Toxicol Appl Pharmacol* 2006; **216**: 98–107.
62. Liu ZX, Han D, Gunawan B, Kaplowitz N. Neutrophil depletion protects against murine acetaminophen hepatotoxicity. *Hepatology* 2006; **43**: 1220–30.
63. Jaeschke H, Liu J. Neutrophil depletion protects against murine acetaminophen hepatotoxicity: another perspective. *Hepatology* 2007; **45**: 1588–9; author reply 89.
64. Bajt ML, Yan HM, Farhood A, Jaeschke H. Plasminogen activator inhibitor-1 limits liver injury and facilitates regeneration after acetaminophen overdose. *Toxicol Sci* 2008; **104**: 419–27.
65. Holt MP, Cheng L, Ju C. Identification and characterization of infiltrating macrophages in acetaminophen-induced liver injury. *J Leukoc Biol* 2008; **84**: 1410–21.
66. Senoo H, Kojima N, Sato M. Vitamin A-storing cells (stellate cells). *Vitam Horm* 2007; **75**: 131–59.
67. Straub BK, Stoeffel P, Heid H, Zimbelmann R, Schirmacher P. Differential pattern of lipid droplet-associated proteins and de novo perilipin expression in hepatocyte steatogenesis. *Hepatology* 2008; **47**: 1936–46.
68. Nagatsuma K, Hayashi Y, Hano H, *et al.* Lecithin: retinol acyltransferase protein is distributed in both hepatic stellate cells and endothelial cells of normal rodent and human liver. *Liver Int* 2009; **29**: 47–54.
69. Mezaki Y, Yoshikawa K, Yamaguchi N, *et al.* Rat hepatic stellate cells acquire retinoid responsiveness after activation in vitro by post-transcriptional regulation of retinoic acid receptor alpha gene expression. *Arch Biochem Biophys* 2007; **465**: 370–9.
70. Yoshikawa K, Imai K, Seki T, *et al.* Distribution of retinyl ester-storing stellate cells in the arrowtooth halibut, Atheresthes evermanni. *Comp Biochem Physiol A Mol Integr Physiol* 2006; **145**: 280–6.
71. Wold HL, Wake K, Higashi N, *et al.* Vitamin A distribution and content in tissues of the lamprey, Lampetra japonica. *Anat Rec* 2004; **276**: 134–42.
72. Irie T, Kajiwara S, Kojima N, Senoo H, Seki T. Retinal is the essential form of retinoid for storage and transport in the adult of the ascidian Halocynthia roretzi. *Comp Biochem Physiol B Biochem Mol Biol* 2004; **139**: 597–606.
73. Bonis PA, Friedman SL, Kaplan MM. Is liver fibrosis reversible? *N Engl J Med* 2001; **344**: 452–4.
74. Desmet VJ, Roskams T. Cirrhosis reversal: a duel between dogma and myth. *J Hepatol* 2004; **40**: 860–7.
75. Rockey DC, Maher JJ, Jarnagin WR, Gabbiani G, Friedman SL. Inhibition of rat hepatic lipocyte activation in culture by interferon-gamma. *Hepatology* 1992; **16**: 776–84.
76. Maubach G, Lim MC, Kumar S, Zhuo L. Expression and upregulation of cathepsin S and other early molecules required for antigen presentation in activated hepatic stellate cells upon IFN-gamma treatment. *Biochim Biophys Acta* 2007; **1773**: 219–31.
77. Yavrom S, Chen L, Xiong S, *et al.* Peroxisome proliferator-activated receptor gamma suppresses proximal alpha1(I) collagen promoter via inhibition of p300-facilitated NF-I binding to DNA in hepatic stellate cells. *J Biol Chem* 2005; **280**: 40650–9.
78. Cheng JH, She H, Han YP, *et al.* Wnt antagonism inhibits hepatic stellate cell activation and liver fibrosis. *Am J Physiol Gastrointest Liver Physiol* 2008; **294**: G39–49.
79. Klein I, Cornejo JC, Polakos NK, *et al.* Kupffer cell heterogeneity: functional properties of bone marrow derived and sessile hepatic macrophages. *Blood* 2007; **110**: 4077–85.
80. Azzi A, Gysin R, Kempna P, *et al.* Regulation of gene expression by alpha-tocopherol. *Biol Chem* 2004; **385**: 585–91.
81. Kinoshita K, Iimuro Y, Otogawa K, *et al.* Adenovirus-mediated expression of BMP-7 suppresses the development of liver fibrosis in rats. *Gut* 2007; **56**: 706–14.
82. Friedman SL. Seminars in medicine of the Beth Israel Hospital, Boston. The cellular basis of hepatic fibrosis. Mechanisms and treatment strategies. *N Engl J Med* 1993; **328**: 1828–35.
83. Gressner AM, Bachem MG. Molecular mechanisms of liver fibrogenesis – a homage to the role of activated fat-storing cells. *Digestion* 1995; **56**: 335–46.
84. Olaso E, Friedman SL. Molecular regulation of hepatic fibrogenesis. *J Hepatol* 1998; **29**: 836–47.
85. Kawada N. The hepatic perisinusoidal stellate cell. *Histol Histopathol* 1997; **12**: 1069–80.
86. Okuyama H, Shimahara Y, Kawada N. The hepatic stellate cell in the post-genomic era. *Histol Histopathol* 2002; **17**: 487–95.
87. Kim Y, Ratziu V, Choi SG, *et al.* Transcriptional activation of transforming growth factor beta1 and its receptors by the Kruppel-like factor Zf9/core promoter-binding protein and Sp1. Potential mechanisms for autocrine fibrogenesis in response to injury. *J Biol Chem* 1998; **273**: 33750–8.
88. Dey A, Cederbaum AI. Alcohol and oxidative liver injury. *Hepatology* 2006; **43**: S63–74.
89. Ramm GA, Ruddell RG. Hepatotoxicity of iron overload: mechanisms of iron-induced hepatic fibrogenesis. *Semin Liver Dis* 2005; **25**: 433–49.
90. Kato J, Kobune M, Nakamura T, *et al.* Normalization of elevated hepatic 8-hydroxy-2′-deoxyguanosine levels in chronic hepatitis C patients by phlebotomy and low iron diet. *Cancer Res* 2001; **61**: 8697–702.

91. Kawada N, Kristensen DB, Asahina K, *et al.* Characterization of a stellate cell activation-associated protein (STAP) with peroxidase activity found in rat hepatic stellate cells. *J Biol Chem* 2001; **276**: 25318–23.
92. Nakatani K, Okuyama H, Shimahara Y, *et al.* Cytoglobin/STAP, its unique localization in splanchnic fibroblast-like cells and function in organ fibrogenesis. *Lab Invest* 2004; **84**: 91–101.
93. Xu R, Harrison PM, Chen M, *et al.* Cytoglobin overexpression protects against damage-induced fibrosis. *Mol Ther* 2006; **13**: 1093–100.
94. Ogawa T, Tateno C, Asahina K, *et al.* Identification of vitamin A-free cells in a stellate cell-enriched fraction of normal rat liver as myofibroblasts. *Histochem Cell Biol* 2007; **127**: 161–74.
95. Magness ST, Bataller R, Yang L, Brenner DA. A dual reporter gene transgenic mouse demonstrates heterogeneity in hepatic fibrogenic cell populations. *Hepatology* 2004; **40**: 1151–9.
96. Knolle PA, Gerken G. Local control of the immune response in the liver. *Immunol Rev* 2000; **174**: 21–34.
97. Crispe IN. Hepatic T cells and liver tolerance. *Nat Rev Immunol* 2003; **3**: 51–62.
98. Polakos NK, Cornejo JC, Murray DA, *et al.* Kupffer cell-dependent hepatitis occurs during influenza infection. *Am J Pathol* 2006; **168**: 1169–78; quiz 404–5.
99. Tu Z, Bozorgzadeh A, Pierce RH, *et al.* TLR-dependent cross talk between human Kupffer cells and NK cells. *J Exp Med* 2008; **205**: 233–44.
100. Dunn C, Brunetto M, Reynolds G, *et al.* Cytokines induced during chronic hepatitis B virus infection promote a pathway for NK cell-mediated liver damage. *J Exp Med* 2007; **204**: 667–80.
101. Geissmann F, Cameron TO, Sidobre S, *et al.* Intravascular immune surveillance by CXCR6$^+$ NKT cells patrolling liver sinusoids. *PLoS Biol* 2005; **3**: e113.
102. Eksteen B, Grant AJ, Miles A, *et al.* Hepatic endothelial CCL25 mediates the recruitment of CCR9$^+$ gut-homing lymphocytes to the liver in primary sclerosing cholangitis. *J Exp Med* 2004; **200**: 1511–7.
103. Adams DH, Eksteen B. Aberrant homing of mucosal T cells and extra-intestinal manifestations of inflammatory bowel disease. *Nat Rev Immunol* 2006; **6**: 244–51.
104. Curbishley SM, Eksteen B, Gladue RP, Lalor P, Adams DH. CXCR 3 activation promotes lymphocyte transendothelial migration across human hepatic endothelium under fluid flow. *Am J Pathol* 2005; **167**: 887–99.
105. Schrage A, Wechsung K, Neumann K, *et al.* Enhanced T cell transmigration across the murine liver sinusoidal endothelium is mediated by transcytosis and surface presentation of chemokines. *Hepatology* 2008; **48**: 1262–72.
106. Bertolino P, Trescol-Biemont MC, Rabourdin-Combe C. Hepatocytes induce functional activation of naive CD8$^+$ T lymphocytes but fail to promote survival. *Eur J Immunol* 1998; **28**: 221–36.
107. Bowen DG, Zen M, Holz L, *et al.* The site of primary T cell activation is a determinant of the balance between intrahepatic tolerance and immunity. *J Clin Invest* 2004; **114**: 701–12.
108. Callery MP, Kamei T, Flye MW. Kupffer cell blockade inhibits induction of tolerance by the portal venous route. *Transplantation* 1989; **47**: 1092–4.
109. Winau F, Hegasy G, Weiskirchen R, *et al.* Ito cells are liver-resident antigen-presenting cells for activating T cell responses. *Immunity* 2007; **26**: 117–29.
110. Limmer A, Ohl J, Kurts C, *et al.* Efficient presentation of exogenous antigen by liver endothelial cells to CD8$^+$ T cells results in antigen-specific T-cell tolerance. *Nat Med* 2000; **6**: 1348–54.
111. Bertolino P, Schrage A, Bowen DG, *et al.* Early intrahepatic antigen-specific retention of naive CD8$^+$ T cells is predominantly ICAM-1/LFA-1 dependent in mice. *Hepatology* 2005; **42**: 1063–71.
112. Diehl L, Schurich A, Grochtmann R, *et al.* Tolerogenic maturation of liver sinusoidal endothelial cells promotes B7-homolog 1-dependent CD8$^+$ T cell tolerance. *Hepatology* 2008; **47**: 296–305.
113. Limmer A, Ohl J, Wingender G, *et al.* Cross-presentation of oral antigens by liver sinusoidal endothelial cells leads to CD8 T cell tolerance. *Eur J Immunol* 2005; **35**: 2970–81.
114. Berg M, Wingender G, Djandji D, *et al.* Cross-presentation of antigens from apoptotic tumor cells by liver sinusoidal endothelial cells leads to tumor-specific CD8(+) T cell tolerance. *Eur J Immunol* 2006; **36**: 2960–70.
115. Jessup JM, Battle P, Waller H, *et al.* Reactive nitrogen and oxygen radicals formed during hepatic ischemia-reperfusion kill weakly metastatic colorectal cancer cells. *Cancer Res* 1999; **59**: 1825–9.
116. Anasagasti MJ, Alvarez A, Avivi C, Vidal-Vanaclocha F. Interleukin-1-mediated $H_2O_2$ production by hepatic sinusoidal endothelium in response to B16 melanoma cell adhesion. *J Cell Physiol* 1996; **167**: 314–23.
117. Bayon LG, Izquierdo MA, Sirovich I, *et al.* Role of Kupffer cells in arresting circulating tumor cells and controlling metastatic growth in the liver. *Hepatology* 1996; **23**: 1224–31.
118. Timmers M, Vekemans K, Vermijlen D, *et al.* Interactions between rat colon carcinoma cells and Kupffer cells during the onset of hepatic metastasis. *Int J Cancer* 2004; **112**: 793–802.
119. Vekemans K, Timmers M, Vermijlen D, *et al.* CC531s colon carcinoma cells induce apoptosis in rat hepatic endothelial cells by the Fas/FasL-mediated pathway. *Liver Int* 2003; **23**: 283–93.
120. Jessup JM, Samara R, Battle P, Laguinge LM. Carcinoembryonic antigen promotes tumor cell survival in liver through an IL-10-dependent pathway. *Clin Exp Metastasis* 2004; **21**: 709–17.
121. Mendoza L, Carrascal T, De Luca M, *et al.* Hydrogen peroxide mediates vascular cell adhesion molecule-1 expression from interleukin-18-activated hepatic sinusoidal endothelium: implications for circulating cancer cell arrest in the murine liver. *Hepatology* 2001; **34**: 298–310.
122. Vidal-Vanaclocha F, Fantuzzi G, Mendoza L, *et al.* IL-18 regulates IL-1beta-dependent hepatic melanoma metastasis via vascular cell adhesion molecule-1. *Proc Natl Acad Sci USA* 2000; **97**: 734–9.
123. Auguste P, Fallavollita L, Wang N, *et al.* The host inflammatory response promotes liver metastasis by increasing tumor cell arrest and extravasation. *Am J Pathol* 2007; **170**: 1781–92.
124. Mendoza L, Valcarcel M, Carrascal T, *et al.* Inhibition of cytokine-induced microvascular arrest of tumor cells by recombinant endostatin prevents experimental hepatic melanoma metastasis. *Cancer Res* 2004; **64**: 304–10.
125. Wang N, Thuraisingam T, Fallavollita L, *et al.* The secretory leukocyte protease inhibitor is a type 1 insulin-like growth factor receptor-regulated protein that protects against liver metastasis by attenuating the host proinflammatory response. *Cancer Res* 2006; **66**: 3062–70.
126. Zubia A, Mendoza L, Vivanco S, *et al.* Application of stereocontrolled stepwise [3+2] cycloadditions to the preparation of inhibitors of alpha(4)beta(1)-integrin-mediated hepatic melanoma metastasis. *Angew Chem Int Ed Engl* 2005; **44**: 2903–7.
127. Olaso E, Salado C, Egilegor E, *et al.* Proangiogenic role of tumor-activated hepatic stellate cells in experimental melanoma metastasis. *Hepatology* 2003; **37**: 674–85.
128. Mueller L, Goumas FA, Affeldt M, *et al.* Stromal fibroblasts in colorectal liver metastases originate from resident fibroblasts and generate an inflammatory microenvironment. *Am J Pathol* 2007; **171**: 1608–18.
129. Vermeulen PB, Colpaert C, Salgado R, *et al.* Liver metastases from colorectal adenocarcinomas grow in three patterns with different angiogenesis and desmoplasia. *J Pathol* 2001; **195**: 336–42.
130. Solaun MS, Mendoza L, De Luca M, *et al.* Endostatin inhibits murine colon carcinoma sinusoidal-type metastases by preferential targeting of hepatic sinusoidal endothelium. *Hepatology* 2002; **35**: 1104–16.

*Am J Physiol Regul Integr Comp Physiol* 294: R311–R320, 2008.
First published November 21, 2007; doi:10.1152/ajpregu.00735.2007.

# Attenuation of acute and chronic liver injury in rats by iron-deficient diet

**Kohji Otogawa,[1]* Tomohiro Ogawa,[1]* Ryoko Shiga,[2] Kazuki Nakatani,[2] Kazuo Ikeda,[2] Yuji Nakajima,[2] and Norifumi Kawada[1]**

*Departments of [1]Hepatology and [2]Anatomy, Graduate School of Medicine, Osaka City University, Osaka, Japan*

Submitted 9 October 2007; accepted in final form 15 November 2007

**Otogawa K, Ogawa T, Shiga R, Nakatani K, Ikeda K, Nakajima Y, Kawada N.** Attenuation of acute and chronic liver injury in rats by iron-deficient diet. *Am J Physiol Regul Integr Comp Physiol* 294: R311–R320, 2008. First published November 21, 2007; doi:10.1152/ajpregu.00735.2007.—Oxidative stress due to iron deposition in hepatocytes or Kupffer cells contributes to the initiation and perpetuation of liver injury. The aim of this study was to clarify the association between dietary iron and liver injuries in rats. Liver injury was initiated by the administration of thioacetamide or ligation of the common bile duct in rats fed a control diet (CD) or iron-deficient diet (ID). In the acute liver injury model induced by thioacetamide, serum levels of aspartate aminotransferase and alanine aminotransferase, as well as hepatic levels of lipid peroxide and 4-hydroxynonenal, were significantly decreased in the ID group. The expression of 8-hydroxydeoxyguanosine and terminal deoxynucleotidyl transferase biotin-dUTP nick-end labeling positivity showed a similar tendency. The expression of interleukin-1β and monocyte chemotactic protein-1 mRNA was suppressed in the ID group. In liver fibrosis induced by an 8-wk thioacetamide administration, ID suppressed collagen deposition and smooth muscle α-actin expression. The expressions of collagen 1A2, transforming growth factor β, and platelet-derived growth factor receptor β mRNA were all significantly decreased in the ID group. Liver fibrosis was additionally suppressed in the bile-duct ligation model by ID. In culture experiments, deferoxamine attenuated the activation process of rat hepatic stellate cells, a dominant producer of collagen in the liver. In conclusion, reduced dietary iron is considered to be beneficial in improving acute and chronic liver injuries by reducing oxidative stress. The results obtained in this study support the clinical usefulness of an iron-reduced diet for the improvement of liver disorders induced by chronic hepatitis C and alcoholic/nonalcoholic steatohepatitis.

oxidative stress; fibrosis; stellate cell; Kupffer cell

IN GENERAL, THE METABOLISM, uptake, and excretion of iron in the body are strictly regulated (1, 7, 33). The majority of iron in the body is contained in erythrocytes as a component of hemoglobin and circulates throughout the whole body to allow vital biological processes. Most of the other iron is stored in the spleen and liver as a component of iron-containing enzymes such as cytochrome *P*-450. However, the presence of free iron and deposition of iron in cells often occurs under some pathological conditions, triggering oxidative stress and inflammation (4, 24, 30). For instance, hemochromatosis and iron-overload due to the excessive intake of iron-containing medicine and supplements frequently induce liver cell damage and, in some cases, cirrhosis (2, 31).

It has been shown that the deposition of iron occurs frequently in some liver diseases, including viral hepatitis (3, 6), alcoholic liver injury (5, 38), and nonalcoholic steatohepatitis (NASH) (8, 36). Iron reduction by phlebotomy reduced mean serum alanine transaminase (ALT) activity and induced disappearance of iron deposits in the liver in chronic active hepatitis C patients (9, 13). Thus, iron is considered to play a role in the onset of liver cell damage. Free iron induces the production of proinflammatory and fibrogenic mediators such as TNF-α and transforming growth factor β (TGF-β) and nuclear factor-κB (NF-κB) activation in hepatic macrophages (17, 35, 39). Recently, we showed that the phagocytosis of erythrocytes by hepatic macrophages results in the deposition of iron derived from hemoglobin in the liver and contributes to the pathogenesis of NASH in a rabbit model (29). In that study, we clearly showed that iron reduction by phlebotomy lowers iron deposition in the liver and spleen and attenuates the progression of liver fibrosis.

Free metal ions are known to be important for the production of free radicals, among which iron is most potent in vivo (24, 30). The generated free radicals induce lipid peroxidation, DNA breakage, and 8-hydroxy-2′-deoxyguanosine (8-OHdG) formation, resulting in tissue damage and DNA mutagenesis (11, 18, 37). Although it has been clarified that iron overload may be associated with hepatitis, cirrhosis, or liver cancer, it is still unclear whether an iron-restricted diet has protective effects against acute liver injury and fibrosis. We have postulated that hepatic iron depletion contributes to the attenuation of liver injury caused in rats by the administration of the hepatotoxin thioacetamide (TAA).

Herein, we showed that iron depletion has the potential to attenuate acute liver damage and fibrosis in rats induced by TAA and ligation of the common bile duct. Analysis of this mechanism revealed that iron depletion hampers oxidative stress, inflammation, and hepatic stellate cell activation, resulting in the inhibition of liver fibrosis.

## MATERIALS AND METHODS

*Animals.* Pathogen-free male Wistar rats were obtained from SLC (Shizuoka, Japan). Animals were housed at a constant temperature and supplied with laboratory chow and water ad libitum. The experimental protocol was approved by the Animal Research Committee of Osaka City University (Guide for Animal Experiments, Osaka City University).

*Animal models.* Rats weighing 200 to 230 g were fed a control diet (CD; $n = 5$) or an iron-deficient diet (ID; $n = 5$; Oriental Yeast, Tokyo, Japan) for 4 wk. The contents of the CD and ID are shown in Table 1. Successively, the rats were intraperitoneally administered TAA (100 mg/body wt; Wako, Osaka, Japan) to produce an acute liver failure model. Rats were killed to excise the liver at 48 h after TAA administration. Alternatively, the survival of rats with acute

* Kohji Otogawa and Tomohiro Ogawa contributed equally to this study.
Address for reprint requests and other correspondence: N. Kawada, Dept. of Hepatology, Graduate School of Medicine, Osaka City Univ., 1-4-3, Asahimachi, Abeno, Osaka 545-8585, Japan (e-mail: kawadanori @med.osaka-cu.ac.jp).

The costs of publication of this article were defrayed in part by the payment of page charges. The article must therefore be hereby marked "*advertisement*" in accordance with 18 U.S.C. Section 1734 solely to indicate this fact.

Table 1. *Nutrition contents of control and iron-deficient diets*

| Nutrition Contents | Control Diet | Iron-Deficient Diet |
|---|---|---|
| Total fat, % | 6.4 | 6.4 |
| Soy protein, % | 27.5 | 27.5 |
| Total carbohydrates, % | 46.6 | 46.6 |
| Salt mixture, % | 8.1 | 8.1 |
| Iron, mg/100 g | 12.3 | 0.03 |
| Fiber, % | 4.1 | 4.1 |
| Moisture, % | 6.9 | 6.9 |

The other contents, including copper and vitamins, were equilibrated.

liver failure induced by TAA administration (60 mg/body wt) was observed in CD ($n = 15$) and ID ($n = 15$) groups until 4 days.

As a liver fibrosis model, rats were supplied with CD ($n = 5$) or ID ($n = 5$) for 4 wk and successively intraperitoneally administrated with TAA (50 mg/body wt) twice a week for 6 wk (26).

*Preparation of hepatic stellate cells.* Hepatic stellate cells were isolated from male Wistar rats, as previously described (20). Isolated stellate cells were cultured on plastic dishes in DMEM containing 10% FCS and antibiotics (DMEM/FCS). On *day 2* of primary culture, the medium was replaced by DMEM/FCS with or without test agents, and the culture was continued for another 3 days. Then, the cells were prepared for morphological observation, immunoblotting, immunostaining, and a thymidine-incorporation assay.

*Determination of serum concentrations of iron, aspartate aminotransferase, alanine aminotransferase, and lipid peroxide.* Blood was collected from the inferior vena cava and centrifuged at 3,000 rpm for 10 min at room temperature. Serum concentrations of iron, aspartate aminotransferase (AST), ALT, and lipid peroxide (LPO) were measured at Special Reference Laboratories (SRL; Osaka, Japan).

*Determination of hepatic iron and LPO.* The liver of each animal was perfused via the portal vein with PBS to remove the blood. The hepatic free iron concentration and LPO were measured at SRL. The free iron concentration in the liver was measured by Nitroso-PSAP method.

*Histochemical and immunohistochemical staining.* The liver of each animal was perfused through the portal vein with PBS to remove the blood and then fixed with 4% paraformaldehyde or Bouin's fluid. The liver tissues were embedded, cut into 5-μm-thick sections, and then underwent hematoxylin and eosin and Sirius red staining, as described previously (19). Immunostaining using monoclonal antibodies against 8-OHdG (Japan Institute for the Control of Aging (JaICA), Shizuoka, Japan) and smooth muscle α-actin (αSMA; Sigma Chemical, St. Louis, MO) was performed according to the methods described previously (29).

*Terminal deoxynucleotidyl transferase-mediated deoxyuridine triphosphate nick-end labeling staining.* For the detection of apoptosis, paraffin sections were stained by the terminal deoxynucleotidyl transferase-mediated deoxyuridine triphosphate nick-end labeling (TUNEL) technique using an in situ apoptosis detection kit (Takara, Shiga, Japan), according to the manufacturer's instructions.

*Determination of caspase-3 and -8 activities.* Caspase-3 and -8 activities were determined using the caspase-3 and -8 colorimetric assay kits (Biovision, Mountain View, CA), respectively, as previously described (25) according to the manufacturer's recommendation.

*Immunoblotting.* Protein samples (10 μg) were subjected to SDS-PAGE, and then transferred onto Immobilon P membranes (Millipore, Bedford, MA) (22). After blocking, the membranes were treated with primary antibodies against 4-hydroxy-2-nonenal (4-HNE; JaICA), platelet-derived growth factor receptor β (PDGFRβ, Santa Cruz Biotechnology, Santa Cruz, CA), αSMA, ERK1/2 (Cell Signaling Technology, Beverly, MA), phospho-ERK1/2 ($Thr^{202}/Tyr^{204}$) (Cell Signaling Technology), Akt (Cell Signaling Technology), and phospho-Akt ($Ser^{473}$) (Cell Signaling Technology), and then were incubated with peroxidase-conjugated secondary antibodies. Immunoreactive bands were visualized using the enhanced chemiluminescence system (Amersham Pharmacia Biotech, Little Chalfont, Buckinghamshire, UK) and with an LAS 1000 (Fuji Photo Film, Kanagawa, Japan). The density of bands was analyzed using a Bio-Rad GS-700 densitometer (Bio-Rad, Hercules, CA).

*Real-time RT-PCR.* Total RNAs for the RT-PCR were extracted from the livers using the RNeasy total RNA system (Qiagen, Hilden, Germany). cDNAs were synthesized using 1 μg of total RNA, ReverTra Ace (Toyobo, Osaka, Japan), and $Oligo(dT)_{12-18}$ primer according to the manufacturer's instructions. The expression levels of genes were measured by real-time RT-PCR using the cDNAs, real-time PCR master mix (Toyobo), and a set of gene-specific oligonucleotide primers and the TaqMan probe listed in Table 2.

*[$^3$H]Thymidine-incorporation assay.* Isolated stellate cells were cultured on plastic dishes for 2 days in DMEM/FCS. The medium was then replaced by DMEM/FCS with or without deferoxamine (Sigma Chemical, St. Louis, MO). The culture was continued for one more day and pulse-labeled with 1.0 μCi/ml [$^3$H]thymidine during the last 6 h. The incorporated radioactivity was subjected to liquid scintillation counting, as previously described (22).

*Statistical analysis.* Data presented as bar graphs are the means ± SD of at least three independent experiments. Statistical analysis was performed by Student's *t*-test ($P < 0.01$ was considered significant). Kaplan-Meier survival analysis was used for survival data obtained by the log-rank test and Wilcoxon test.

Table 2. *List of primer sequences*

| Genes | Forward Primers (5′-3′) | Reverse Primers (5′-3′) | TaqMan Probes (5′-3′) | Accession No. |
|---|---|---|---|---|
| αSMA | GAGGAGCATCCGACCTTGC | TTTCTCCCGGTTGGCCTTA | AACGGAGGCGCCGCTGAACC | NM_031004 |
| TGFβ1 | TGCTTCCGCATCACCGT | TAGTAGACGATGGGCAGTGGC | CTGCGTGCCGCAGGCTTTGG | NM_021578 |
| PDGFRβ | ACGGCACTCAGGGTACACCT | AAGGGACCAGTTCTAGGACTCGT | ACAGGAAGCACCCACTCCTTTTAGCCC | NM_031525 |
| IL-1β | CTTCCCCAGGACATGCTAGG | CAAAGGCTTCCCCTGGAGAC | AGCCCCCTTGTCGAGAATGGGC | NM_031512 |
| MCP-1 | CAGATGCAGTTAATGCCCCAC | AGCCGACTCATTGGGATCAT | CACCTGCTGCTACTCATTCACTGGCAA | M57441 |
| IL-6 | TGTCTCGAGCCCACCAGG | TGCGGAGAGAAACTTCATAGCTG | CGAAAGTCAACTCCATCTGCCCTTCAGG | NM_012589 |
| TNF-α | GCTCCCTCTCATCAGTTCCATG | TACGGGCTTGTCACTCGAGTTTTG | CCCAGACCCTCACACTCAGATCATCTTC | NM_012675 |
| COL1A2 | AAGGGTCCTTCTGGAGAACC | TCGAGAGCCAGGGAGACCCA | CAGGGTCTTCTTGGTGCTCCCGGTAT | NM_053356 |
| TIMP-2 | GCCCTATGATCCCATGCTAC | TGCCCATTGATGCTCTTCTCT | CTCCCCGGATGAGTGCCTCTGGA | L31884 |
| MMP-2 | CCCCATGAAGCCTTGTTTACC | TTGTAGGAGGTGCCCTGGAA | AATGCTGATGGACAGCCCTGCA | NM_031054 |
| GAPDH | AAGATGGTGAAGGTCGGTGTG | GAAGGCAGCCCTGGTAACC | CGGATTTGGCCGTATCGGACGC | NM_017008 |

αSMA, smooth muscle α-actin; TGFβ1, transforming growth factor β1; PDGFRβ, platelet-derived growth factor receptor β; MCP-1, monocyte chemotactic protein-1; COL1A2, collagen1A2; TIMP-2, tissue inhibitor of matrix metalloproteinase-2 (MMP-2).

## RESULTS

*Suppression of acute liver injury by an iron-deficient diet.* The iron-deficient diet significantly reduced the content of iron in the liver (CD: 12.7 ± 0.6 μg/100 mg vs. ID: 1.3 ± 0.6 μg/100 mg) and the serum (CD: 175.0 ± 5.0 μg/dl vs. ID: 72.3 ± 3.7 μg/dl), as shown in Fig. 1*A*. Single-shot TAA (100 mg/body wt)-induced hepatocyte damage indicated by serum levels of AST and ALT were clearly reduced in the ID group (Fig. 1*B*). Alternatively, observation of the survival of rats with acute liver failure induced by daily TAA administration (60 mg/body wt) indicated that all CD-fed rats died within 3 days after starting TAA administration, whereas 87% of ID-fed rats survived until 4 days of TAA (Fig. 1*C*).

*Decrease of hepatocyte apoptosis by iron-deficient diet.* In the acute liver injury model, hepatocyte injury was observed around the central vein in the CD group (Fig. 2*A*), while lipid degeneration was observed in a few hepatocytes in the ID group (Fig. 2*B*). TUNEL-positive cells were rare in the ID group compared with the CD group (Fig. 2, *C* and *D*). Activities of both caspase-3 and -8 in liver homogenates were lower in the ID group (Fig. 2*E*).

*Decrease of oxidative stress by iron-deficient diet.* Acute liver injury caused oxidative DNA damage in hepatocytes, as revealed by the appearance of 8-OHdG in the nuclei (Fig. 3*A*). 8-OHdG-positive hepatocytes were abundant in the CD group, whereas they were scarce in the ID group (Fig. 3*B*). Alterna-

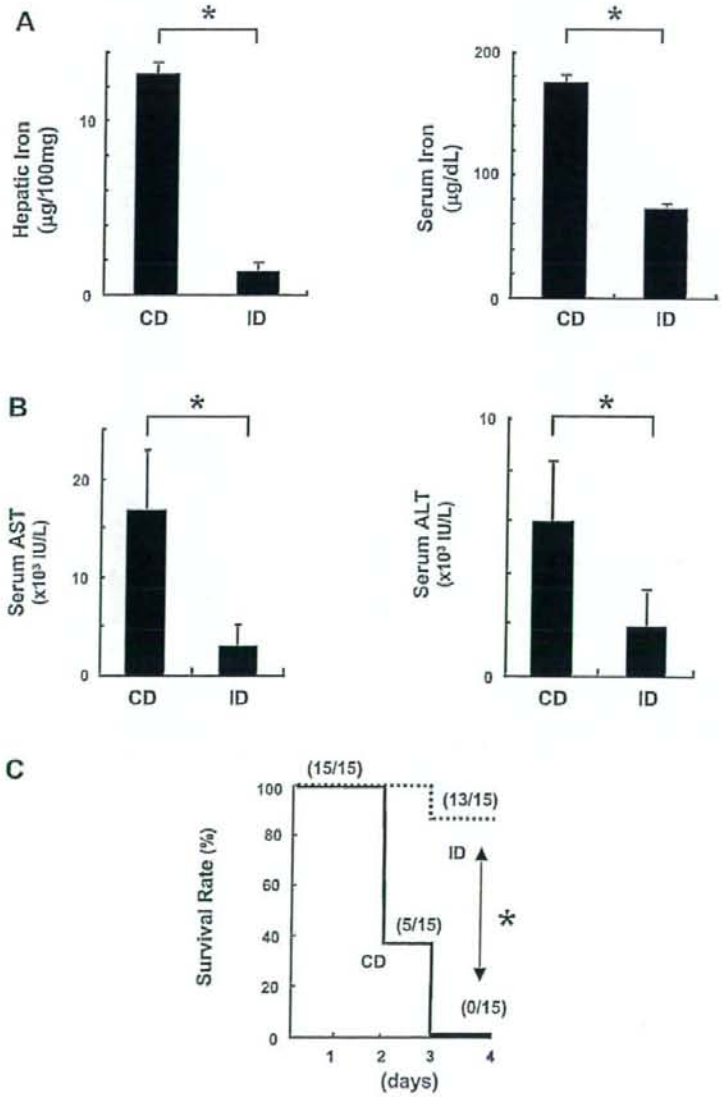


Fig. 1. Effect of iron-deficient diet on acute liver injury. *A*: free iron levels in the serum and liver. Significant differences in the levels of free iron were found in both serum and liver between the control diet (CD; $n = 5$) and the iron-deficient diet (ID; $n = 5$) rats. $^*P < 0.01$. *B*: levels of aspartate aminotransferase (AST; *left*) and alanine transaminase (ALT; *right*) in serum at 48 h after thioacetamide (TAA) administration (100 mg/body). Significant differences were found in the levels of both AST and ALT between CD ($n = 5$) and ID ($n = 5$) rats. $^*P < 0.01$. *C*: survival curves in the TAA-induced acute liver failure model. Rats were fed CD or ID for 4 wk. Successively, TAA (60 mg/body) was administrated to the rats every day. Survival was observed until 4 days after starting TAA administration. $^*P < 0.01$.

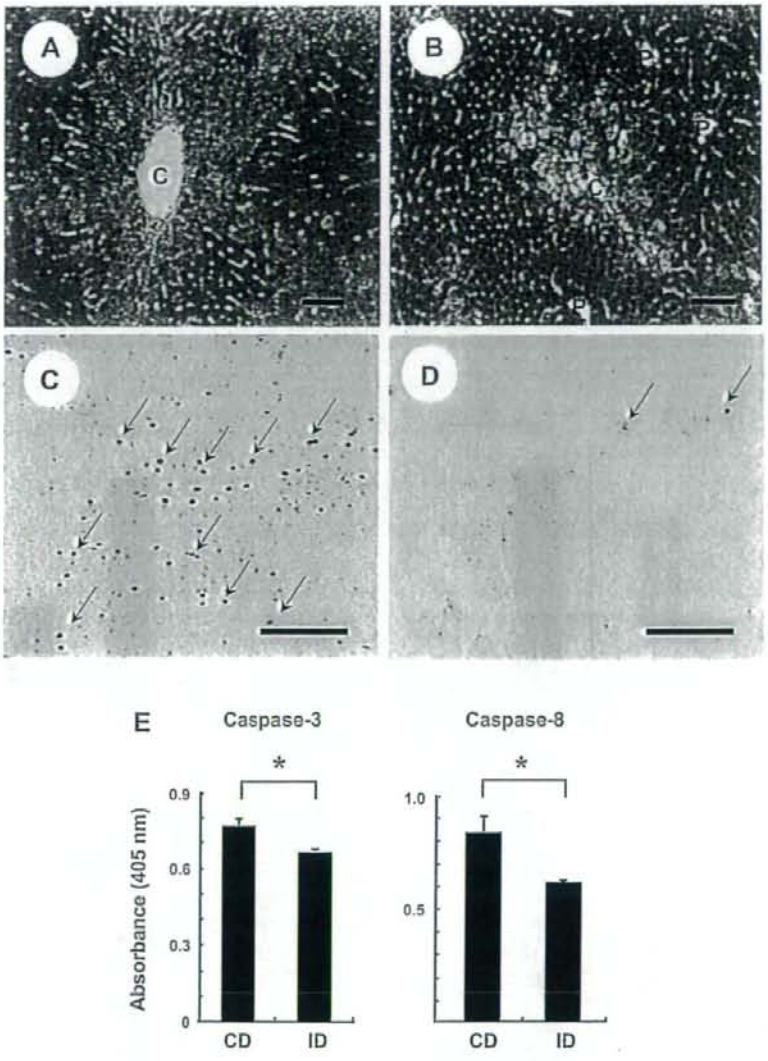


Fig. 2. Detection of apoptosis in the liver. *A*, *B*: hematoxylin and eosin (H&E) staining of the liver. *A*: CD group. *B*: ID group. Note that hepatocyte degeneration is clear in the CD group compared with the ID group. P, portal vein; C, central vein. *C*, *D*: Terminal deoxynucleotidyl transferase biotin-dUTP nick-end labeling (TUNEL) staining. *C*: CD group. *D*: ID group. Note that TUNEL-positive cells (arrows) are abundant in the CD group, whereas they are scarce in the ID group. *E*: activity of caspases in the liver. Caspase-3 and -8 activities were determined using the Caspase-3 and -8 colorimetric assay kits, respectively. Note that activity of the caspases was significantly reduced in the ID group. $*P < 0.01$. Scale bars: 100 μm.

tively, expression of 4-HNE, an a, b-unsaturated hydroxyalkene, which is produced by lipid peroxidation in cells and is one of the oxidative products, was clearly decreased in the liver homogenate of the ID group, as revealed by Western blot analysis (Fig. 3*C*). In addition, LPO, an oxidative degradation product of polyunsaturated fatty acids, was significantly reduced both in the serum and liver by ID administration (Fig. 3*D*).

*Changes in mRNA expression of inflammatory and fibrogenetic genes in acute liver injury.* Quantitative RT-PCR analyses revealed that the expressions of inflammatory genes such as IL-1β, monocyte chemotactic protein-1 (MCP-1), IL-6, and TNF-α were all significantly suppressed in the ID group. Expressions of mRNAs of TGF-β1, PDGFRβ, tissue inhibitor of matrix metalloproteinase-2 (TIMP-2), and matrix metalloproteinase-2 (MMP-2) were also significantly reduced in the ID group, although mRNA expressions of smooth muscle α-actin and collagen 1A2, which are markers of the activation of stellate cells, were not significantly changed (Fig. 4).

*Effect of iron-deficient diet on liver fibrosis induced by TAA.* Next, the effect of an iron-deficient diet on liver fibrosis induced by the repetitive injection of TAA into rats was examined. As shown in Fig. 5*A*, a macroscopic view of the liver of a CD-fed rat injected with TAA (100 mg/body wt, twice a week) for 6 wk showed a nodular surface, indicative of liver cirrhosis. In contrast, liver surfaces were smooth and nearly intact in the ID-fed group (Fig. 5*B*). Sirius Red staining of the liver revealed the development of micronodules and macronodules surrounded by collagen fibers in the CD group (Fig. 5*C*), while in the ID group, faint fibrosis was seen only around the central veins (Fig. 5*D*). Immunohistochemistry also indicated that αSMA-positive myofibroblasts were abundant in the CD group, while they were scarce in the ID group (Fig. 5,

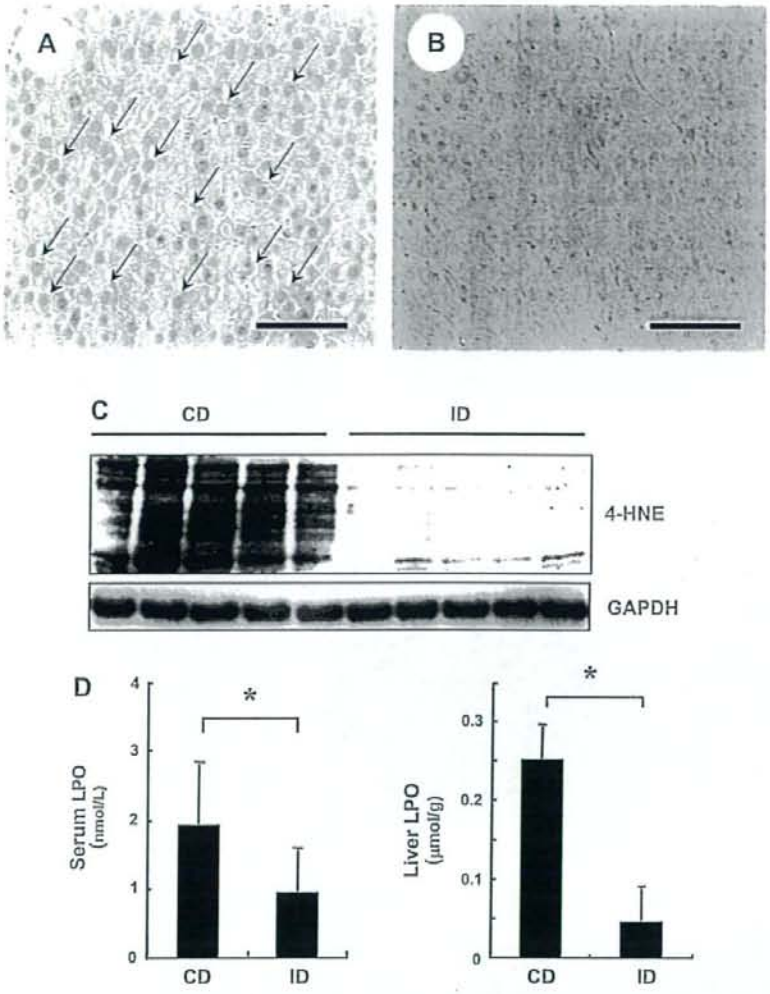


Fig. 3. Detection of oxidative stress in the liver. *A*, *B*: 8-hydroxy-2-deoxy guanosine (8-OHdG) staining of the liver. *A*: CD group. *B*: ID group. Note that 8-OHdG expression in hepatocytes is clear in the CD group (arrows) compared with the ID group. *C*: 4-Hydroxy-2-nonenal (4-HNE) expression in the liver. Liver homogenates were applied to Western blot analysis using anti-4-HNE antibodies. Note that 4-HNE was detected in proteins over a broad range of molecular weights in the CD group, while it was scarce in the ID group. *D*: serum and liver lipid peroxide (LPO) levels in the CD group and ID group. $^*P <$ 0.01. Scale bars: 100 μm.

*E* and *F*), clearly showing that the activation of stellate cells and myofibroblasts was inhibited in the ID group. At this stage, serum levels of AST and ALT were lower in the ID group than in the CD group (data not shown).

*Changes in mRNA expression of inflammatory and fibrogenetic genes in chronic liver injury.* Quantitative RT-PCR analyses revealed that the expressions of fibrosis-related genes such as αSMA, TGF-β1, PDGFRβ, collagen 1A2, TIMP-2, and MMP-2 were all clearly reduced in the ID group. In contrast to the acute liver injury model, expressions of MCP-1, IL-6, and TNF-α were unchanged. The expression of IL-1β mRNA was augmented in the ID group (Fig. 6).

*Effect of iron-deficient diet on liver fibrosis induced by common bile duct ligation.* To test whether the attenuation of liver fibrosis development by ID was reproduced in another liver fibrosis model, we used a common bile duct ligation model. In this model, hepatocyte degeneration and deposition of collagen fibers were seen in the portal vein area, whose histology sharply contrasted to the fibrosis induced by TAA (Fig. 7, *A* and *C*). As shown in Fig. 7, *B* and *D*, hepatocyte degeneration and the deposition of collagen fibers were clearly suppressed in the ID group.

*Effect of deferoxamine on stellate cell activation.* The results mentioned above indicate that iron may play critical roles in the occurrence of liver fibrosis, as well as acute liver injury. Recent experimental reports have revealed that hepatic stellate cells have multiple roles in the inflammatory and fibrotic responses accompanying their own activation process. Therefore, in the last series in this study, we tested the effects of deferoxamine ($C_{25}H_{48}N_6O_8$), a specific chelator of iron, otherwise known as desferrioxamine or desferal, on stellate cell function during their activation, because the removal of iron molecules from serum-containing medium is technically difficult.

As shown in Fig. 8*A*, *a*, rat stellate cells isolated and cultured for 5 days in the serum-containing medium adhered to the plastic plate and extended their cytoplasmic processes. Lipid particles, which contain vitamin A, localized around enlarged

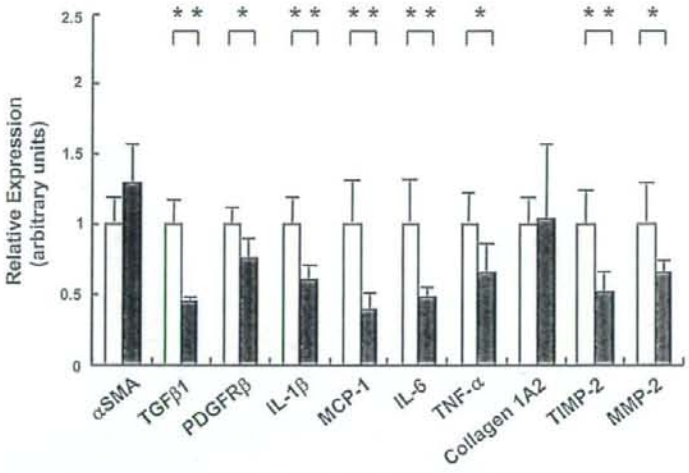


Fig. 4. Expression of inflammatory and fibrogenetic genes in the TAA-induced acute liver failure model in CD and ID groups. Total RNAs were extracted under the condition of TAA-induced acute liver failure in the CD group (white) and ID group (gray) and were subjected to real-time RT-PCR. αSMA, smooth muscle α-actin. $*P < 0.05$; $**P < 0.01$.

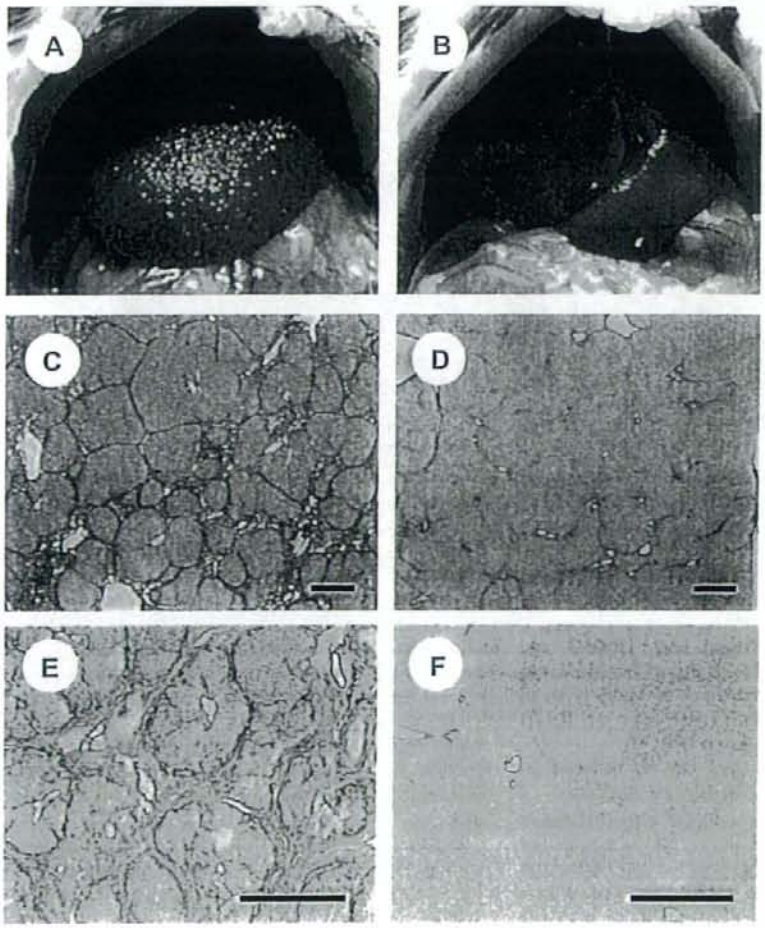


Fig. 5. Effect of an iron-deficient diet on liver fibrosis induced by TAA. *A*, *B*: macroscopic view of the liver of rats injected with TAA for 6 wk in the CD group (*left*) and ID group (*right*). *C*, *D*: Sirius Red staining in the CD group (*left*) and ID group (*right*). *E*, *F*: immunostaining of smooth muscle α-actin in the CD group (*left*) and ID group (*right*). Scale bars: 500 μm.

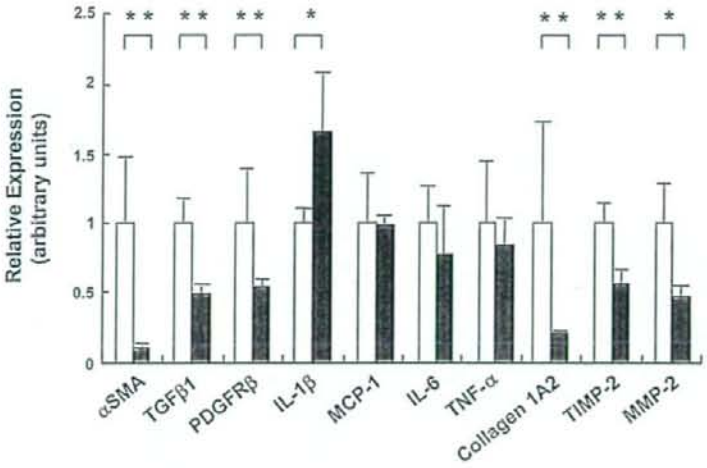


Fig. 6. Expression of inflammatory and fibrotic genes on liver fibrosis induced by TAA in CD group and ID group. Total RNAs were extracted from liver fibrosis induced by TAA in CD group (white) and ID group (gray) for real-time RT-PCR. Note that the expression of all fibrotic genes [smooth muscle α-actin (αSMA), transforming growth factor β1 (TGFβ1), platelet-derived growth factor receptor β (PDGFRβ) collagen 1A2, and tissue inhibitor of matrix metalloproteinase-2 (MMP-2) (TIMP-2)] was inhibited in the ID group. $*P < 0.05$; $**P < 0.01$.

nuclei, some of which were undergoing the process of multiplication. When they were incubated in identical medium supplemented with $10^{-4}$ M deferoxamine, they maintained the quiescent phenotype with dendritic processes and small nuclei (Fig. 8*A*, *b*).

The expression of markers for stellate cell activation, such as PDGFRβ and smooth muscle α-actin, was suppressed by deferoxamine in a dose-dependent manner, as revealed by Western blot analysis (Fig. 8*B*). In fact, immunofluorescence staining of αSMA confirmed the results of Western blot analysis (Fig. 8*C*).

Finally, deferoxamine inhibited [$^3$H]thymidine uptake by stellate cells in a dose-dependent manner (Fig. 8*D*), and PDGF-BB-stimulated phosphorylation of ERK and Akt (Fig. 8*E*).

## DISCUSSION

The role of iron in the pathophysiology of the liver has long been studied in fields of hemochromatosis (2, 31) and alcoholic liver injury (5, 38). Recently, an unusual accumulation of iron in the liver has also been observed in chronic hepatitis C (3, 6) and nonalcoholic steatohepatitis (8, 36). Thus, research on iron homeostasis and dysregulation in the liver is one of the topics in the research field of hepatology. The upregulation and downregulation of hepcidin production by hepatocytes under pathological conditions regulates the absorption of iron from the small intestine, a process considered to represent the most important pathway (21, 23). However, medicines that regulate hepcidin production

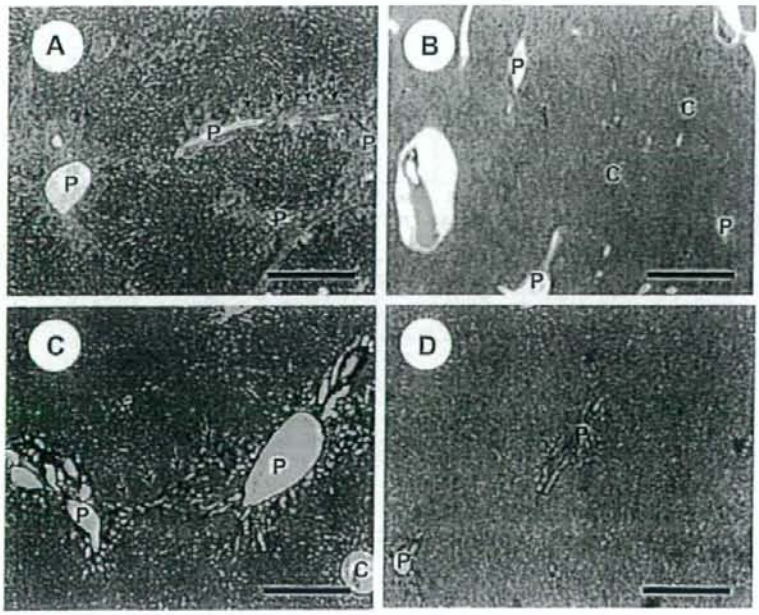


Fig. 7. Effect of iron-deficient diet on liver fibrosis induced by ligation of the common bile duct. *A*, *B*: H&E staining of the liver. *A*: CD group. *B*: ID group. Note that hepatocyte degeneration around the portal vein area is clear in the CD group compared with the ID group. P, portal vein; C, central vein. *C*, *D*: Sirius Red staining. *C*: CD group. *D*: ID group. Note that collagen deposition extended around the portal vein area in the CD group, while it was reduced in the ID group. P, portal vein; C, central vein. Arrows indicate P-P bridge formation. Scale bars: 1 mm.

have not been discovered. Phlebotomy is a relatively safe and convenient therapy to deprive iron from the body (9, 13). Body iron can be reduced by phlebotomy by 50 mg iron/100 ml. However, to maintain a low iron level, repeat phlebotomy is required, which is inconvenient for patients. In this regard, iron-chelating therapy (15, 28) and an iron-deficient diet can replace the need for phlebotomy. In particular, the clinical use of ICL670 (deferasirox), an orally administrable $Fe^{3+}$-chelator, in hepatic iron overload is now awaited (14, 16).

To study the effectiveness of an iron-deficient diet in the attenuation of liver injuries, we tested the effect of a low iron diet on acute and chronic liver injuries induced by TAA administration. In acute liver injury, the iron-deficient diet protected rats from liver damage and failure and improved their survival (Fig. 1). Mechanistic analyses revealed that iron depletion reduced apoptosis of hepatocytes, presumably through attenuating the activation of caspase-3 and -8 (Fig. 2). Additionally, as expected, iron depletion suppressed 8-OHdG expression in hepatocytes, as well as the expression of 4-HNE and LPO in liver tissue, indicating the role of iron in the occurrence of oxidative stress (Fig. 3). The accepted explanation for iron-induced oxidative stress is that it is caused by the Fenton pathway, which generates the hydroxyradical (·OH), a strongly reactive radical molecule (1, 7, 24, 33). This hydroxyradical modulates DNA, proteins, sugars, and biomembranes, resulting in the damage of cellular functions (4, 24, 30). Alternatively, it can be speculated that the hepatic iron increase, which probably takes place in the current TAA model, could explain protective role of iron-deficient diet. A previous report by Oliver et al. (27) indicated that the identical treatment itself resulted in increase of hepatic iron in metallothionein-I/II knockout mice. Thus, it may be speculated that iron levels will not be elevated to the same levels in iron-deficient rats compared with rats on a complete diet.

Hepatic stellate cells play pivotal roles in inflammatory and fibrotic processes in the liver (10, 32, 34). In particular, in response to oxidative stress and cytokines, including TGF-β and PDGF-BB, they change their cellular characteristics from a vitamin A-storing phenotype to matrix-producing and smooth muscle α-actin-expressing phenotypes resembling myofibroblasts present in the organs (12). The synthesis and secretion of type I collagen is upregulated, resulting in the contribution of fibrotic septum formation in the chronically inflamed liver. The activation process is triggered by oxygen free radicals, including hydrogen peroxide ($H_2O_2$), which can be produced by the Fenton reaction of $Fe^{2+} + H_2O_2 \rightarrow Fe^{3+} + {\cdot}HO + HO^-$. Thus, free iron may induce the activation of stellate cells, indicating that iron removal or a reduction in its content in and around stellate cells may attenuate the progression of liver fibrosis. In

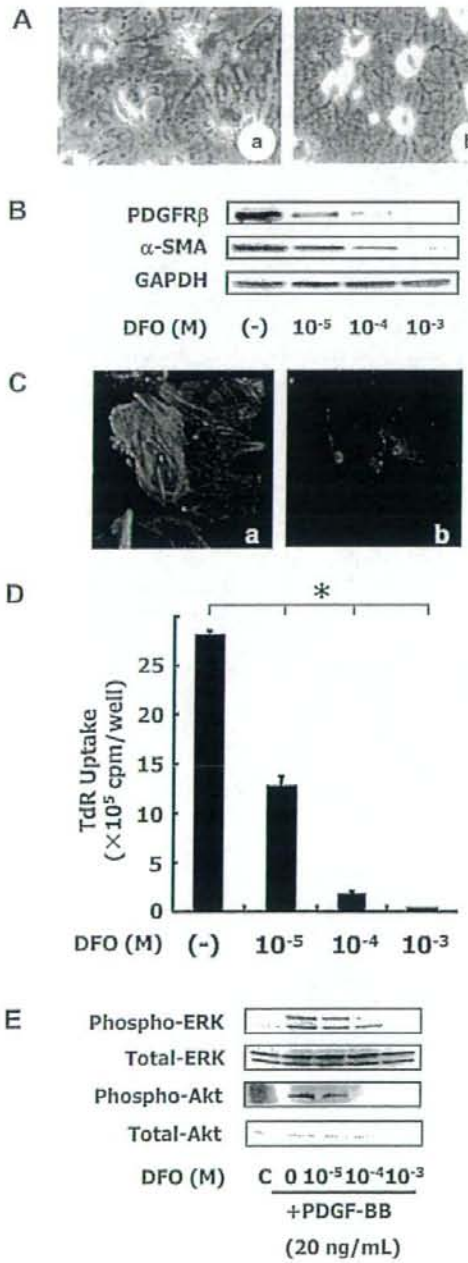


Fig. 8. Effect of deferoxamine on the activation of rat stellate cells in culture. Rat stellate cells were isolated and plated on plastic plates in serum-containing medium. At 24 h after plating, deferoxamine was added to the culture medium at the indicated concentration. *A*: morphology of stellate cells 5 days after plating. *a*: control. *b*: deferoxamine-treated cells. *B*: expression of PDGFRβ and smooth muscle α-actin in stellate cells 5 days after plating. Western blot analysis. Note that deferoxamine dose-dependently suppressed the expression of PDGFRβ and smooth muscle α-actin. DFO, deferoxamine. *C*: immunostaining of smooth muscle α-actin in stellate cells. *a*: control. *b*: deferoxamine ($10^{-4}$ M)-treated cells. Note that stress fibers consisting of smooth muscle α-actin are well developed in nontreated control cells, while they are not organized in deferoxamine-treated cells. *D*: DNA synthesis of stellate cells. DNA synthesis was determined by the [$^3$H]thymidine incorporation assay. Note that deferoxamine suppressed DNA synthesis of stellate cells in a dose-dependent manner. *E*: effect of deferoxamine on PDGF-BB-stimulated activation of ERK and Akt pathways. Stellate cells were cultured for 5 days in the presence or absence of deferoxamine. Then, they were stimulated with PDGF-BB (20 ng/ml) for 10 min. Harvested cells were subjected to Western blot analysis to detect phospho-ERK, total ERK, phospho-Akt, and total Akt. Note that deferoxamine suppressed the phosphorylation of ERK and Akt in a dose-dependent manner.

fact, rats receiving the iron-deficient diet showed marked attenuation of the progression of liver fibrosis (Fig. 5). This is considered to have resulted from the reduction of hepatocyte damage and by the inhibition of stellate cell activation. This assumption may be supported by the results obtained using deferoxamin, showing that iron chelation inhibited the expression of PDGFRβ and αSMA, their proliferation, and PDGF-BB-dependent signal cascades such as ERK and Akt (Fig. 8).

The role of Kupffer cells in the attenuation of liver damage by an iron-deficient diet should also be considered. Iron has been reported as a critical factor for the regulation of Kupffer cell activation with respect to alcoholic liver disease (35, 39). Ionic iron ($Fe^{2+}$) is reported to activate NF-κB, resulting in the enhanced production of TNF-α (35, 39). In this study, we observed the reduction of mRNA expression via iron-deficient diet administration of IL-1β, MCP-1, IL-6, and TNF-α, all of which are NF-κB-dependent genes (Fig. 4). Although we did not determine the free iron content in Kupffer cells, reduction of the iron content in the liver hampers NF-κB and inflammatory gene expression.

### *Perspectives and Significance*

An iron-deficient diet is effective in reducing hepatocyte damage in the acute liver injury model and in the attenuation of liver fibrosis in the chronic model. Attenuation of hepatocyte apoptosis is considered to be caused by the reduction of oxidative stress and decrease of inflammatory gene expression. Furthermore, iron is speculated to be a key molecule in the progression of stellate cell activation and ECM gene expression. The control of iron homeostasis in the liver can be a therapeutic strategy for chronic liver disorder.

### ACKNOWLEDGMENTS

The authors thank to Ms. Michiko Ohashi for her technical assistance. This study was supported by a Grant-In-Aid for Scientific Research from the Japan Society for the Promotion of Science (to N. Kawada).

### REFERENCES

1. **Aisen P, Enns C, and Wessling-Resnick M.** Chemistry and biology of eukaryotic iron metabolism. *Int J Biochem Cell Biol* 33: 940–959, 2001.
2. **Beutler E, Hoffbrand AV, Cook JD.** Iron deficiency and overload. *Hematology Am Soc Hematol Educ Program* 40–61, 2003.
3. **Bonkovsky HL, Banner BF, Rothman AL.** Iron and chronic viral hepatitis. *Hepatology* 25: 759–768, 1997.
4. **Caro AA, Cederbaum AI.** Oxidative stress, toxicology, and pharmacology of CYP2E1. *Annu Rev Pharmacol Toxicol* 44: 27–42, 2004.
5. **Dey A, Cederbaum AI.** Alcohol and oxidative liver injury. *Hepatology* 43: S63-S74, 2006.
6. **Di Bisceglie AM, Axiotis CA, Hoofnagle JH, Bacon BR.** Measurements of iron status in patients with chronic hepatitis. *Gastroenterology* 102: 2108–2113, 1992.
7. **Eisenstein RS.** Iron regulatory proteins and the molecular control of mammalian iron metabolism. *Annu Rev Nutr* 20: 627–662, 2000.
8. **Fargion S, Mattioli M, Fracanzani AL, Sampietro M, Tavazzi D, Fociani P, Taioli E, Valenti L, Fiorelli G.** Hyperferritinemia, iron overload, and multiple metabolic alterations identify patients at risk for nonalcoholic steatohepatitis. *Am J Gastroenterol* 96: 2448–2455, 2001.
9. **Fontana RJ, Israel J, LeClair P, Banner BF, Tortorelli K, Grace N, Levine RA, Fiarman G, Thiim M, Tavill AS, Bonkovsky HL.** Iron reduction before and during interferon therapy of chronic hepatitis C: results of a multicenter, randomized, controlled trial. *Hepatology* 31: 730–736, 2000.
10. **Friedman SL.** Seminars in medicine of the Beth Israel Hospital, Boston. The cellular basis of hepatic fibrosis Mechanisms and treatment strategies. *N Engl J Med* 328: 1828–1835, 1993.
11. **Fujita N, Horiike S, Sugimoto R, Tanaka H, Iwasa M, Kobayashi Y, Hasegawa K, Ma N, Kawanishi S, Adachi Y, Kaito M.** Hepatic oxidative DNA damage correlates with iron overload in chronic hepatitis C patients. *Free Radic Biol Med* 42: 353–362, 2007.
12. **Galli A, Svegliati-Baroni G, Ceni E, Milani S, Ridolfi F, Salzano R, Tarocchi M, Grappone C, Pellegrini G, Benedetti A, Surrenti C, Casini A.** Oxidative stress stimulates proliferation and invasiveness of hepatic stellate cells via a MMP2-mediated mechanism. *Hepatology* 41: 1074–1084, 2005.
13. **Hayashi H, Takikawa T, Nishimura N, Yano M, Isomura T, Sakamoto N.** Improvement of serum aminotransferase levels after phlebotomy in patients with chronic active hepatitis C and excess hepatic iron. *Am J Gastroenterol* 89: 986–988, 1994.
14. **Hershko C, Konijn AM, Nick HP, Breuer W, Cabantchik ZI, Link G.** ICL670A: a new synthetic oral chelator: evaluation in hypertransfused rats with selective radioiron probes of hepatocellular and reticuloendothelial iron stores and in iron-loaded rat heart cells in culture. *Blood* 97: 1115–1122, 2001.
15. **Hoffbrand AV, Gorman A, Laulicht M, Garidi M, Economidou J, Georgipoulou P, Hussain MA, Flynn DM.** Improvement in iron status and liver function in patients with transfusional iron overload with long-term subcutaneous desferrioxamine. *Lancet* 1: 947–949, 1979.
16. **Ibrahim AS, Gebermariam T, Fu Y, Lin L, Husseiny MI, French SW, Schwartz J, Skory CD, Edwards JE, Spellberg BJ.** The iron chelator deferasirox protects mice from mucormycosis through iron starvation. *J Clin Invest* 117: 2649–2657, 2007.
17. **Ishizaka N, Saito K, Noiri E, Sata M, Ikeda H, Ohno A, Ando J, Mori I, Ohno M, Nagai R.** Administration of ANG II induces iron deposition and upregulation of TGF-beta1 mRNA in the rat liver. *Am J Physiol Regul Integr Comp Physiol* 288: R1063–R1070, 2005.
18. **Kato J, Kobune M, Nakamura T, Kuroiwa G, Takada K, Takimoto R, Sato Y, Fujikawa K, Takahashi M, Takayama T, Ikeda T, Niitsu Y.** Normalization of elevated hepatic 8-hydroxy-2′-deoxyguanosine levels in chronic hepatitis C patients by phlebotomy and low iron diet. *Cancer Res* 61: 8697–8702, 2001.
19. **Kinoshita K, Iimuro Y, Otogawa K, Saika S, Inagaki Y, Nakajima Y, Kawada N, Fujimoto J, Friedman SL, Ikeda K.** Adenovirus-mediated expression of BMP-7 suppresses the development of liver fibrosis in rats. *Gut* 56: 706–714, 2007.
20. **Kristensen DB, Kawada N, Imamura K, Miyamoto Y, Tateno C, Seki S, Kuroki T, Yoshizato K.** Proteome analysis of rat hepatic stellate cells. *Hepatology* 32: 268–277, 2000.
21. **Lee P, Peng H, Gelbart T, Wang L, Beutler E.** Regulation of hepcidin transcription by interleukin-1 and interleukin-6. *Proc Natl Acad Sci USA* 102: 1906–1910, 2005.
22. **Maeda N, Kawada N, Seki S, Arakawa T, Ikeda K, Iwao H, Okuyama H, Hirabayashi J, Kasai K, Yoshizato K.** Stimulation of proliferation of rat hepatic stellate cells by galectin-1 and galectin-3 through different intracellular signaling pathways. *J Biol Chem* 278: 18938–18944, 2003.
23. **Nicolas G, Chauvet C, Viatte L, Danan JL, Bigard X, Devaux I, Beaumont C, Kahn A, Vaulont S.** The gene encoding the iron regulatory peptide hepcidin is regulated by anemia, hypoxia, and inflammation. *J Clin Invest* 110: 1037–1044, 2002.
24. **Okada S.** Iron-induced tissue damage and cancer: the role of reactive oxygen species-free radicals. *Pathol Int* 46: 311–332, 1996.
25. **Okuyama H, Nakamura H, Shimahara Y, Araya S, Kawada N, Yamaoka Y, Yodoi J.** Overexpression of thioredoxin prevents acute hepatitis caused by thioacetamide or lipopolysaccharide in mice. *Hepatology* 37: 1015–1025, 2003.
26. **Okuyama H, Shimahara Y, Kawada N, Seki S, Kristensen DB, Yoshizato K, Uyama N, Yamaoka Y.** Regulation of cell growth by redox-mediated extracellular proteolysis of platelet-derived growth factor receptor beta. *J Biol Chem* 276: 28274–28280, 2001.
27. **Oliver JR, Jiang S, Cherian MG.** Augmented hepatic injury followed by impaired regeneration in metallothionein-I/II knockout mice after treatment with thioacetamide. *Toxicol Appl Pharmacol* 210:190–199, 2006.
28. **Olivieri NF, Brittenham GM, McLaren CE, Templeton DM, Cameron RG, McClelland RA, Burt AD, Fleming KA.** Long-term safety and effectiveness of iron-chelation therapy with deferiprone for thalassemia major. *N Engl J Med* 339: 417–423, 1998.
29. **Otogawa K, Kinoshita K, Fujii H, Sakabe M, Shiga R, Nakatani K, Ikeda K, Nakajima Y, Ikura Y, Ueda M, Arakawa T, Hato F, Kawada N.** Erythrophagocytosis by liver macrophages (Kupffer cells) promotes oxidative stress, inflammation, and fibrosis in a rabbit model of steatohepatitis: implications for the pathogenesis of human nonalcoholic steatohepatitis. *Am J Pathol* 170: 967–980, 2007.

30. **Papanikolaou G, Pantopoulos K.** Iron metabolism and toxicity. *Toxicol Appl Pharmacol* 202: 199–211, 2005.
31. **Pietrangelo A.** Hereditary hemochromatosis-a new look at an old disease. *N Engl J Med* 350: 2383–2397, 2004.
32. **Pinzani M, Marra F.** Cytokine receptors and signaling in hepatic stellate cells. *Semin Liver Dis* 21: 397–416, 2001.
33. **Ponka P.** Tissue-specific regulation of iron metabolism and heme synthesis: distinct control mechanisms in erythroid cells. *Blood* 89: 1–25, 1997.
34. **Ramm GA, Ruddell RG.** Hepatotoxicity of iron overload: mechanisms of iron-induced hepatic fibrogenesis. *Semin Liver Dis* 25: 433–449, 2005.
35. **She H, Xiong S, Lin M, Zandi E, Giulivi C, Tsukamoto H.** Iron activates NF-κB in Kupffer cells. *Am J Physiol Gastrointest Liver Physiol* 283: G719–G726, 2002.
36. **Sumida Y, Nakashima T, Yoh T, Furutani M, Hirohama A, Kakisaka Y, Nakajima Y, Ishikawa H, Mitsuyoshi H, Okanoue T, Kashima K, Nakamura H, Yodoi J.** Serum thioredoxin levels as a predictor of steatohepatitis in patients with nonalcoholic fatty liver disease. *J Hepatol* 38: 32–38, 2003.
37. **Toyokuni S, Sagripanti JL.** Association between 8-hydroxy-2′-deoxyguanosine formation and DNA strand breaks mediated by copper and iron. *Free Radic Biol Med* 20: 859–864, 1996.
38. **Tsukamoto H, Horne W, Kamimura S, Niemela O, Parkkila S, Yla-Herttuala S, Brittenham GM.** Experimental liver cirrhosis induced by alcohol and iron. *J Clin Invest* 96: 620–630, 1995.
39. **Tsukamoto H, Lin M, Ohata M, Giulivi C, French SW, Brittenham G.** Iron primes hepatic macrophages for NF-κB activation in alcoholic liver injury. *Am J Physiol Gastrointest Liver Physiol* 277: G1240–G1250, 1999.

ウイルス肝炎からの発癌の早期発見

# 最も重要な手がかりは肝臓の硬さ

## —肝線維化の新しい検査方法—

小林佐和子・森川浩安・河田則文

大阪市立大学大学院医学研究科肝胆膵病態内科学/こばやし・さわこ　もりかわ・ひろやす　かわだ・のりふみ

### はじめに●

ウイルス性肝炎では，肝線維化の進行が肝癌発症リスクと相関することが知られている．そのため，肝線維化の定量的評価が肝癌の早期発見に直結する可能性がある．現在，臨床的な肝線維化の評価には，肝生検による病理組織診断がgold standardとなっている．しかしながら，肝生検による肝線維化評価では，サンプリングエラーやおのおのの病理診断医による結果の差を考慮する必要があり，定量性に問題がある．また，侵襲的で，疼痛，感染，出血などのリスクを伴うため，反復の検査はむずかしく，長期経過観察のモニタリングには適していない．

近年，このような肝生検のもつ問題点を克服し，さらに非侵襲的に肝線維化を診断する方法として，血液検査，超音波，MRI，CTを用いた新しい検査法が開発されている．本稿ではそれらについて触れてみたい．

### 肝線維化の新しい評価方法●

#### 1. 血液検査

肝線維化の評価には，血小板数，血清線維化マーカー（IV型コラーゲン7S，III型プロコラーゲンN末端ペプチド(P-III-P)，ヒアルロン酸など)が参考にされているが，これら単独で肝線維化をステージ分類させることは困難である．そのため，AAR（AST/ALT比），APRI（AST-to-platelet ratio index），CDS（cirrhosis discriminant score），fibrotest，HALT-Cモデルなど，複数のパラメータを組み合わせた肝線維化予測式がある．HALT-Cモデルは，C型慢性肝炎および肝硬変1,141症例のデータを解析したもので，血小板，INR，AST，ALTなど日常臨床で測定する血液検査データを用いて肝硬変を予測できると報告されている（HALT-C Trial：http://www.haltctrial.org/）．

#### 2. 超音波検査

##### a. FibroScan502®[1)]

体表をピストンで叩打した際に発生する弾性波の肝内進行を超音波装置にて観察することによって，肝線維化を短時間に非侵襲的かつ定量的に測定できるエラストメータFibroScan502®がエコセンス社（フランス）により開発された．通常の体外超音波の要領で右肋間から肝右葉に対して振動波を発振し，弾性度を測定する（図1）．慢性肝疾患における線維化の評価に有用であり，特に，C型肝炎症例においては，肝生検によるMetavir Fibrosis stageや新犬山分類のF stageとの相関が報告されている．われわれの施設でも237例のC型慢性肝炎症例に対して弾性度を測定したところ，F stage 0～4の弾性度（中央値kPa）はそれぞれ4.1，6.3，8.8，14.6，22.2であり，相関が認められた（$p<0.001$）（図2）[2)]．著明な肝萎縮や腹水，肥満などの場合には測定部位の設定が困難な場合もあるが，熟練度を要さず非侵襲的に反復して行うことが可能である．また，肝生検では肝全体の5万分の1しかみていない計算になるが，FibroScan502®では500分の1を反映しているといわれており，より広い範囲の硬度をカバーできる．

##### b. Real-time Tissue Elastography®

われわれのグループでは乳癌診療時に用いるReal-time Tissue Elastography®を用いた肝線維化診断の臨床応用に取り組んでいる．Real-time Tissue Elastography®は日立メディコが開発した日本発の超音波診断法であり，臓器の弾性度を色調により超音波画像として捉えることができる画期的な装置である（図3）．すでに乳腺領域ではその有用性が高く評価され，乳癌検診の精度が大幅に向上することがさまざまな臨床研究で実証さ

1345-1551/08/￥100/頁/JCLS